Preventing, monitoring and curing the ageing in the LHCb Outer Tracker

Erwin Lourens Visser
erwinv@nikhef.nl

July 9, 2010

Masters Thesis
Vrije Universiteit
Faculteit der Exacte Wetenschappen
Particle- and Astroparticle Physics master
De Boelelaan 1081
1081 HV Amsterdam
The Netherlands

Research performed at:
NIKHEF
B-physics group
Science Park 105
1098 XG Amsterdam
The Netherlands

Supervisor: Dr. N. Tuning
Second reader: Dr. H.L. Bethlem

CERN-THESIS-2010-094
09/07/2010

Abstract

The modules of the LHCb Outer Tracker have shown to suffer from gain loss under irradiation at moderate intensities, a process known as ageing. The plastifier in the glue with which the detector modules were constructed, Araldite AY103-1, has been shown to be the culprit. In this thesis this is confirmed by irradiating a module constructed with Araldite AY105-1, which does not contain the harmful plastifier.

Several methods to prevent and repair the gain loss exist. One preventive measure is the addition of oxygen. However, because of its electronegative nature, oxygen can capture some of the drifting electrons, thereby lowering the gain of the OT. Simulations have been done to investigate the effect of oxygen on the gain and efficiency. One method to remove the ageing is HV training. In this procedure the applied voltage is increased such, that the OT enters the discharge regime. These discharges mostly remove the ageing, but can take place anywhere in the straw tube, not necessarily at the location of the ageing. Curing the module while putting a source near the location of the ageing is shown to always cure the gain loss. Finally, a method has been devised to quantify the amount of gain loss in the OT with the standard OT readout electronics. By performing a threshold scan it is possible to accurately determine the average gain loss of the straws.

Contents

List of Tables

List of Figures

Chapter 1

Introduction

The Large Hadron Collider (LHC) is the world's largest and highest-energy particle accelerator [1]. The LHC is located near Geneva, beneath the border between Switzerland and France and consists of four major experiments: ATLAS, CMS, ALICE and LHCb. The ATLAS and CMS experiments will search for the Higgs Boson, the ALICE experiment will look at the quark-gluon plasma, while the LHCb experiment will focus on interactions producing b quarks [2]. More information about the LHCb experiment can be found in section 1.1.

In this thesis I will focus on one of the subdetectors of the LHCb experiment: the Outer Tracker (OT). This subdetector measures particle momenta, which is needed to reconstruct the mass of the decaying B-mesons (mesons containing a b-quark). More information on the OT can be found in section 1.2. The Outer Tracker suffers from signal loss due to radiation, a phenomenon that is known as ageing.

Much is known already about ageing and several methods to reduce and reverse ageing have been developed [3, 4]. However, there are still some unanswered questions about these methods, which I will attempt to answer in this thesis. Section 1.3 gives an overview of the goals of my thesis.

1.1 The LHCb detector

The LHCb experiment is dedicated to b physics at the LHC and its main goals are the high precision study of CP violation and the study of rare B-decays. CP violation plays an important role in cosmology, as this is one of the three ingredients required to explain the imbalance in the amount of matter and antimatter in the universe [5].

After the discovery that both charge conjugation (replacing particles by their antiparticles, abbreviated by C) and parity (inverting the spatial coordinates, abbreviated by P) are maximally violated by the weak interaction, it was thought that the combined operation of C and P would be an exact symmetry of nature. In 1964 it was found however, that CP symmetry is violated in the neutral kaon system [6].

CP violation in the Standard Model is generated by the complex phase of the CKM matrix, which was first introduced by Kobayashi and Maskawa [7]. The amount of CP violation that can be generated in the Standard Model is insufficient to explain the dominance of matter in the

universe. This calls for sources of CP violation generated by new physics.

At first, the CP violation experiments were done in the kaon system, because kaons are produced abundantly due to their low mass. However, the investigation of the heavier B mesons has several advantages, such as the better sensitivity to the CKM matrix elements and the sensitivity to physics beyond the standard model[1]. In order to study B mesons several facilities were constructed, of which the Belle experiment in Japan [8] and Babar in the USA [9] are the most notable. Thanks to the higher beam energy and interaction rate of the LHC, the LHCb experiment can produce a far larger amount of B mesons than the earlier experiments. Besides this, the LHC will also create the heavier B_s mesons, making it the perfect place to study CP violation and new physics.

1.1.1 Detector overview

The LHCb detector consists of several subdetectors [2], and an overview of the detector is shown in figure 1.1. LHCb is a single-arm spectrometer with an angular coverage of 15 to 300 mrad in the bending plane and 15 to 250 mrad in the non-bending plane. Since the magnetic field is oriented along the y-axis and the particles move in the z-direction, the particle tracks are bent in the x-z plane. The detector has been designed this way, since the b- and $\bar{b}$-hadrons are produced predominantly at small angles with respect to the beam pipe.

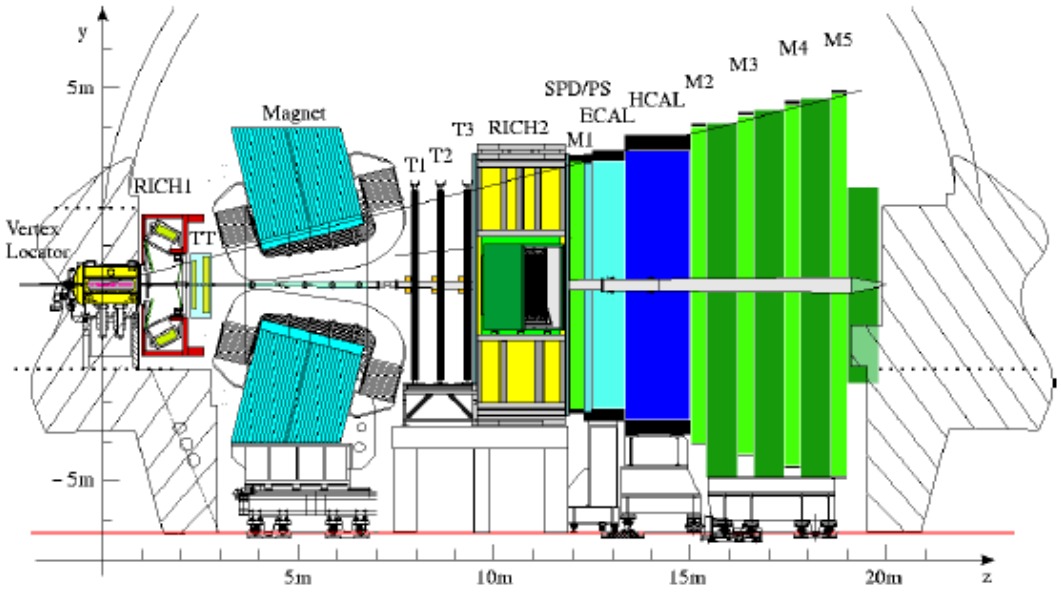

Figure 1.1: *Cross section of the LHCb detector, the interactions take place at y=z=0.*

The collisions take place in the Vertex Locator (VELO), which is shown at the left in figure 1.1. The VELO provides information on the locations of the interaction point and the point where a B-meson decays. The distance between these two points is used to extract the lifetime of

[1]This is done by studying B meson decays that are very rare or even forbidden in the Standard Model.

the produced B-meson. The charged decay products of the B-mesons will then be tracked by the tracking system, the three stations which are marked with T1 – T3 in figure 1.1. The innermost region of each station, which is closest to the beam pipe, is covered with a high resolution silicon detector known as the Inner Tracker (IT). The Outer Tracker covers the remaining part of the station (about 99%). For a detailed picture of the Inner and Outer Tracker, see figure 1.4 in section 1.2. The goal of the tracking system is to reconstruct the tracks of the passing particles, after which the curvature of the tracks can be used to determine their momenta.

Behind the trigger system, the second part of the Ring Imaging Cherenkov (RICH) detector is located. The RICH detector is used to distinguish different charged hadrons. This is done by determining the velocity of the passing particles, which, combined with the momentum measurement of the tracking system gives the mass of the hadrons. The electromagnetic and hadronic calorimeters (ECAL and HCAL respectively) are used to measure the energy of neutral decay products and to trigger on decay products of the B-mesons with high transverse momentum. Finally, the muons are identified in the muon chambers (M1 – M5 in figure 1.1).

1.2 The Outer Tracker

The Outer Tracker is a gas-filled straw tube detector, which works on the principles of a drift chamber. These principles will first be discussed in section 1.2.1, before discussing the OT itself in section 1.2.2 and its readout system in section 1.2.3.

1.2.1 Principles of drift chambers

When a charged particle traverses a gaseous medium it will transfer energy to the gas molecules by electromagnetic interactions. If enough energy is transfered to a molecule, it can be ionized and an electron is liberated. These electrons are called the primary electrons. If the energy of the primary electron is large enough (larger than the ionization potential of the gas), it can further ionize, producing secondary electrons. Since this process takes place over a short range the electrons are created in a cluster. The passing particle creates several clusters. The total ionization is given by the sum of primary and secondary ionizations.

A drift chamber consists of a gas filled region with a cathode and one or more anode wires. A potential is applied to these anode wires, while the cathode is grounded, creating an electric field in the chamber. Due to the presence of the electric field, the ions and electrons will not recombine. Instead, the electrons drift towards the anode wire. When the electric field is high enough (which happens close to the anode wire), the electrons will be sufficiently accelerated to create more elecron-ion pairs. These electrons can in turn create electron-ion pairs causing an avalanche, this process is referred to as gas amplification, and the multiple of electrons created in the avalanche is called gas gain.

Since the electrons have a much lower mass than the ions, their drift velocity will be a few orders of magnitude higher. When the electrons have reached the anode wire, there will be a large cluster of positive ions left near the wire, which will drift towards the cathode. The movement of these ions around the wire will cause a measurable electrical pulse.

Figure 1.2 shows the working principles of a cylindrical drift chamber. In this picture R is the radius of the cell, L is the length of the track in the drift area and r is the distance of closest

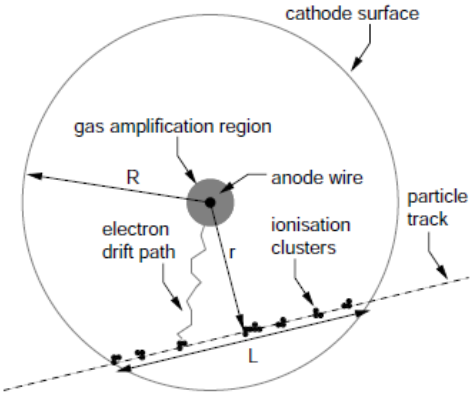

Figure 1.2: *Working principles of a cylindrical drift chamber: a passing charged particle creates several clusters of electrons [10].*

approach of the track. More information on drift chambers can be found in [11, 12].

1.2.2 Outer Tracker schematics

The Outer Tracker consists of cylindrical drift chambers, as described in the previous section, which are called straw tubes. The straw tubes have an inner diameter of 4.9 mm and are wound from two layers of foil material [13]. The inner foil layer, with a thickness of 40 μm, acts as cathode and consists of conductive carbon-doped Kapton XC. The 10 μm thick outer layer is made of Kapton laminated with aluminium and provides shielding between neighbouring channels, thus preventing crosstalk.

The anode wire has a diameter of 25 μm and is made of tungsten with a thin gold layer. Gold, being chemically inactive, protects the wire from chemical reactions in the gas. For the correct determination of the drift time, it is important that the anode wire remains at the centre of the tube. To accomplish this, wire locators are placed at the tube ends and every 80 cm in between. These wire locators are plastic cylinders, centering the wire to a precision better than 100 μm.

The tube will be filled with a gas mixture of $Ar/CO_2/O_2$ 70/28.5/1.5. The main part of the gas mixture comprises a noble gas, in this case argon. A noble gas is chosen since gas amplification is increased due to absence of inelastic scattering of electrons with the gas molecules. Argon is a popular choice because of its low cost.

Besides argon, a so called quencher gas is needed. A quencher is a poly-atomic gas used to absorb photons that are created in the avalanche. If these photons were not removed, they would ionize the cathode. Due to its poly-atomic nature, a quencher can absorb energy via vibrational and rotational states. The quencher gas will also increase the drift time of the electrons, since it reduces the transverse scattering in elastic collisions they make with the atoms of the noble gas. In the OT CO_2 is used as a quencher.

A small amount of oxygen is added to the gas mixture since it has been found to reduce signal loss due to irradiation damage, also known as ageing [4]. Since oxygen is a strong electronegative gas, it will capture a certain percentage of the drifting electrons, thereby lowering the gain.

Simulations have been done to investigate the loss of efficiency for large drift distances, see chapter 3 for more details.

The anode wire will be kept at 1550 V, while the cathode is grounded. At this voltage the OT will be operating in the proportional region, meaning that the output signal is proportional to the charge from the primary ionizations. If higher voltages are applied, above approximately 1850 V [14], the detector enters the discharge region causing unwanted signals and dark currents.

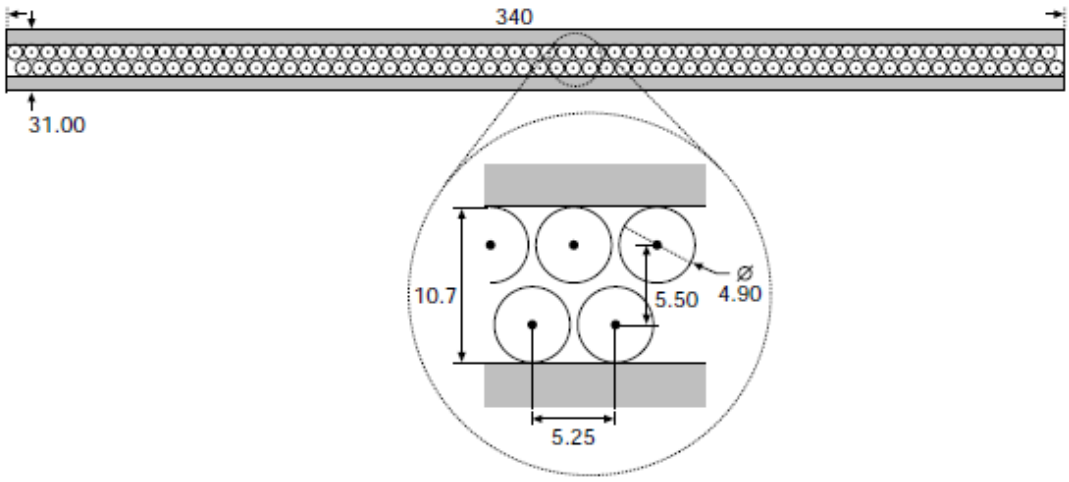

Figure 1.3: *Cross section of an Outer Tracker F module, the inset shows how the straw tubes are arranged. All dimensions are in mm [10].*

A standard OT module (F module) consists of 128 straw tubes, which are placed in two staggered monolayers as shown in figure 1.3. The straw layers are covered with a 1 cm thick panel of Rohacell foam on both sides. On the inside of this panel is a layer of Kapton laminated with aluminium, to which the straws are glued with Araldite AY103-1. To limit channel occupancy[2] the straw tubes are separated at the y=0 plane and are read out separately at the top and the bottom of the module.

Besides the standard F module, 3 other types of modules (S1, S2 and S3) are needed in order to fit the OT closely around the IT and the beam pipe. Figure 1.4 shows the placement of the four different module types in an OT station. All S modules can only be read out from one side, the other side is closed off. The S1 and S2 modules are half the length of the F modules and also contain 128 straws. The S3 modules are half as wide and contain only 64 straws.

Each OT station consists of 4 layers of modules. One of these layers is placed at a stereo angle of -5° with respect to the y-axis, one at an angle of +5° and two with an angle of 0°. This gives information on the y-coordinate at which the particle traverses the station.

Figure 1.5 shows the principle behind track reconstruction in the OT. A charged particle passes through multiple straw tubes, inducing a signal in each of them. The drift time of the electrons depends on the distance of closest approach of the track in each of these tubes. By

[2]The occupancy is the fraction of detector channels that generate a signal in an event. For efficient track reconstruction it must be as low as possible.

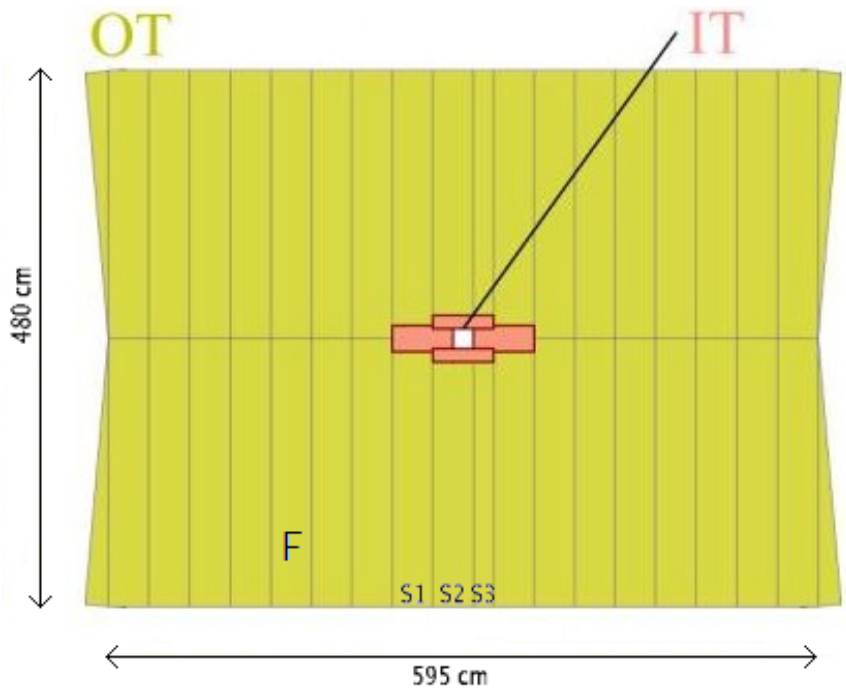

Figure 1.4: *Module arrangement of Outer Tracker modules in one of the three stations. The F and three S module types are shown, the red area in the middle indicates the Inner Tracker.*

measuring these drift times, it is possible to reconstruct the track.

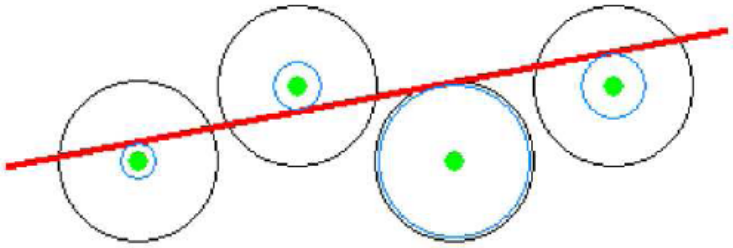

Figure 1.5: *Principle behind track reconstruction. A charged particle passes through four straw tubes. The blue circles denote the distance of closest approach of the track and are a measure for the drift time.*

1.2.3 Outer Tracker readout

As described in section 1.2.1, the output signal of the straw tubes is formed by the movement of the electrons and ions in the gas. The magnitude of the generated signals depends on the energy the charge carriers gain from the electric field per time interval. The electrons only drift a short time, while the drift of the ions to the cathode takes much longer. Because of this, the resulting

signal from a single cluster looks like a short pulse, superimposed on a pulse with a long decay time, as shown in figure 1.6(a).

In reality the signal looks more complicated, because multiple clusters are generated along the track. Also, bunch crossings happen every 25 ns (i.e. at 40 MHz), but the maximum drift times for clusters near the outer edges of the drift area are in the order of 35 ns (see also chapter 3). Because of this, the signals will pile-up, meaning that a new pulse is generated before the effect of the first one has past. To make sure that also the long drifttimes are measured, the straw tubes have a sample window of 75 ns (3 bunch crossings). Figure 1.6(b) shows an output pulse with pile-up from two separate bunch crossings, where both particles create multiple clusters.

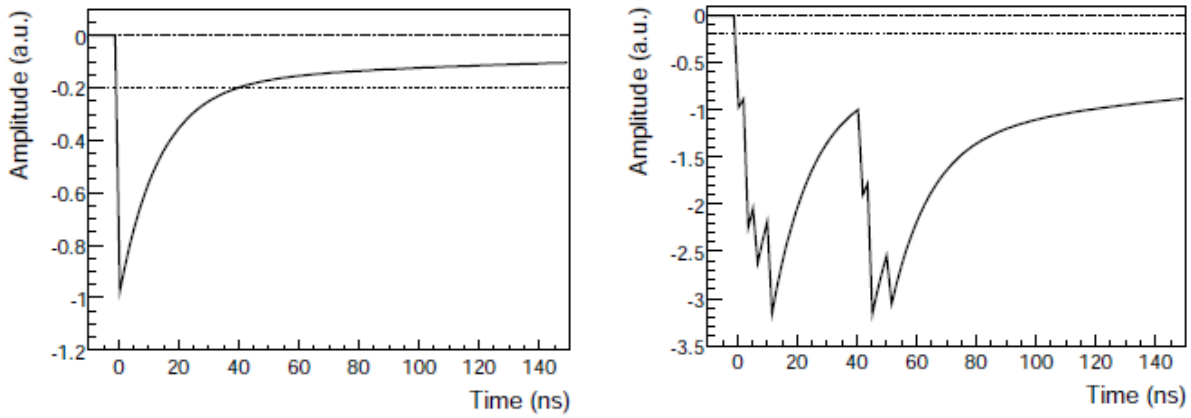

(a) (b)

Figure 1.6: *(a) Output pulse of a straw tube for a single cluster. (b) Pile-up of the pulses from two separate particles, where both particles create multiple clusters.*

The output signals from the straw tubes are read out by a so called preamplifier chip. If the analog signal is above threshold, this chip creates a block pulse which is read by a TDC, which measures the timing of the leading edge. As a preamplifier, the ASDBLR will be used [15], which was developed for the ATLAS TRT detector. ASDBLR stands for Amplifier-Shaper-Discriminator with BaseLine Restoration, a picture is shown in figure 1.7(a). Each ASDBLR chip can read signals from eight straw tubes.

For the timing of the ASDBLR signals, a Time to Digit Converter (TDC) is used. To meet the requirements, a custom TDC was created. It is called the OTIS, which stands for Outer Tracker Time Information System [16]. Each OTIS has 32 input channels, and thus it reads signals from four ASDBLR chips. Since a normal F module contains two layers of 64 channels, four OTIS chips are placed in one Front-End (FE) box mounted on either side of an F-module. The OTIS stores the drift times of all 32 channels in an intermediate memory buffer which will be read out once an L0 trigger[3] is received. Upon a trigger, the data is formatted and transmitted and the buffer is emptied. Besides timing, the OTIS also provides the threshold levels for the ASDBLR chips. A picture of an OTIS board is shown in figure 1.7(b).

[3]The L0 trigger, which is a hardware trigger, reduces the initial rate of 40 MHz down to 1 MHz, only keeping the interesting events.

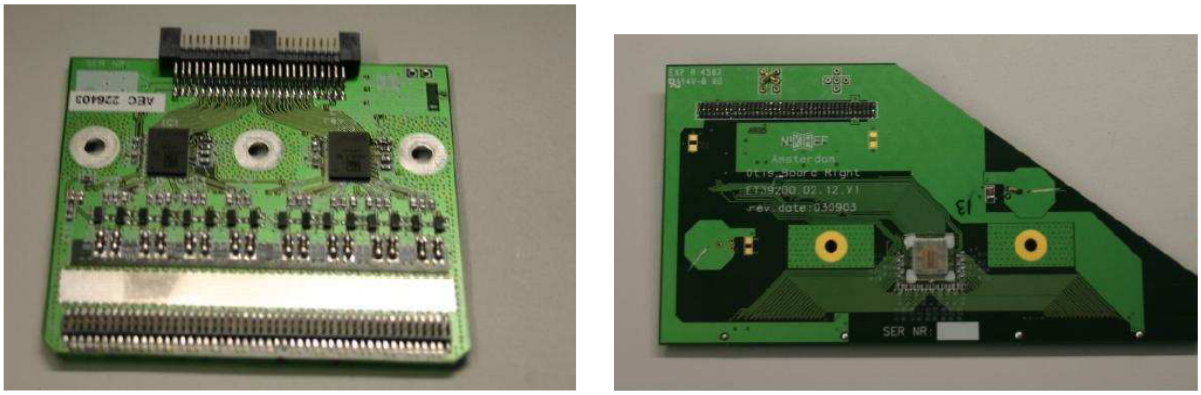

(a) (b)

Figure 1.7: *(a) Picture of a preamplifier board with two ASDBLR chips. (b) Picture of an OTIS TDC board.*

A more detailed description of the OT readout system can be found in [10].

1.3 Goals

The Outer Tracker has shown to suffer from gain loss under irradiation at moderate intensities. Tests during the design phase of the OT only looked at gain loss at high intensities [17], which did not reveal any sign of ageing. Under the influence of low intensity irradiation, a small insulating layer is deposited on the anode wire. This layer consists of molecules created by the outgassing of the glue that is used to construct the modules. The layer reduces the electric field, and hence the amount of detected electrons, thus reducing the detector efficiency. This phenomenon is known as ageing and will be discussed in more depth in chapter 2, together with the present knowledge on the process sofar.

As noted before, the addition of oxygen can reduce the ageing of the OT. Because of its electronegative nature, oxygen can capture some of the drifting electrons, thereby lowering the gain of the OT. Chapter 3 describes the results of simulations of the effect of oxygen on the gain and efficiency.

A number of treatments have been devised to remove the ageing, one of which is HV training. In this procedure the applied voltage is increased such, that the straw tubes enter the discharge regime. These discharges mostly remove the ageing, but can take place anywhere in the straw tube, not necessarily at the location of the ageing. Curing the module while putting a source near the location of the ageing can accomplish a cure of the ageing at the desired location. Results of this method are described in chapter 4.

During detector operation, the pulse heights are not measured since the ASDBLR chip discriminates the incoming pulse against a given value of the threshold. However, using the readout electronics, it is possible to determine the amount of signal loss, by means of a threshold scan without the need to access the detector. This is described in chapter 5.

Chapter 2

Ageing in the Outer Tracker

A general definition of ageing is the decrease of the performance of a detector under the influence of radiation [18]. The Outer Tracker detector of the LHCb experiment suffers from ageing effects by means of reduced signal height, when it is irradiated at moderate intensities. Studies have shown that the plastifier di-isopropyl-naphthalene in the glue used in the construction of the OT modules is the culprit [3].

To detect the presence and the amount of ageing in an OT module, the module is scanned with a ^{90}Sr source before and after it has been irradiated. This method is described in more detail in section 2.1 and will be used extensively in the remainder of this thesis. The characteristics of the ageing phenomenon in the OT will be discussed in section 2.2.

Much research has already been conducted on ageing in the OT and several treatments to prevent and remove ageing have been divised. An overview of these treatments is given in section 2.3.

In order to determine the effect of treatments to remove the effects of ageing, the module in question has to be irradiated first. Various sources in different setups are used to provoque irradiation damage. The intensity profile in most setups is different from that in the real experiment. For this reason, a new setup has been created which resembles the intensity profile of the LHCb detector more closely. The setups used to invoke ageing in the modules will be described in section 2.4.

The plastifier in the glue used to construct the modules is found to be the cause for the ageing problem. To confirm this, a new module has been constructed using glue that does not contain the plastifier, but is otherwise identical. Results from these tests are described in section 2.5.

2.1 Setup

When an OT module is irradiated, traces of the glue plastifier are deposited on the anode wire. This leads to an electrically insulating layer which in turn results in signal loss. The amount of signal loss in an OT module is quantified by measuring the currents in the straws before and after irradiation. This is done by placing the module in a special setup, as shown in figure 2.1(a), and measuring the currents induced by a 20 mCi ^{90}Sr source which is automatically moved along the entire length of the module in steps of 1 cm.

The ^{90}Sr source is located inside the lead casing above the center of the module, irradiating the module through a slit of 1 by 34 cm^2. Since the scanning source is placed above the center of the module, the currents at the edges of the module are lower than those at the center. This can be seen in figure 2.1(b), where the source profile is shown. Since the source is not placed exactly at the center of the module, the source profile is not fully symmetric.

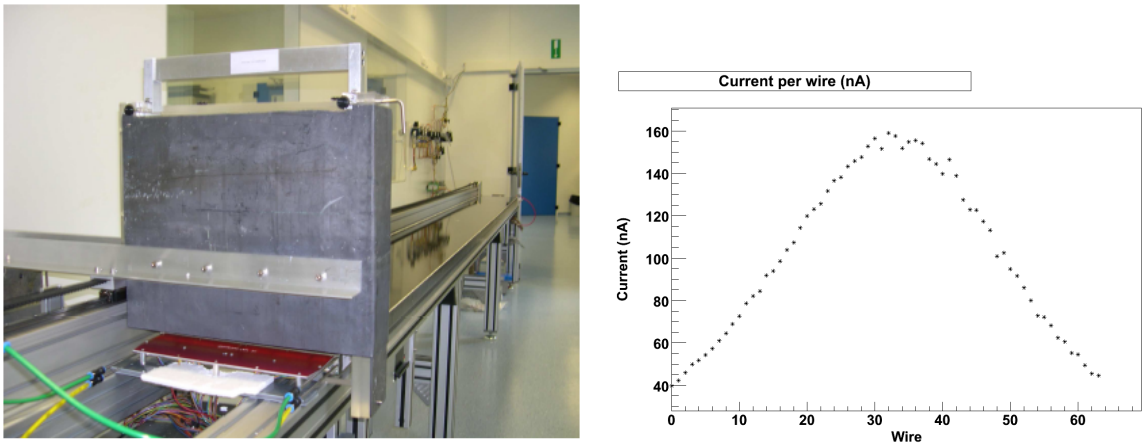

(a) (b)

Figure 2.1: *(a) Picture of the setup with the 20 mCi ^{90}Sr source used to scan an OT module. (b) Source profile of the 20 mCi ^{90}Sr source as measured with an OT module. The profile is measured at a high voltage of 1600 V and with a gasmixture of Ar/CO_2 70/30.*

2.2 Irradiation damage

An example of a ^{90}Sr scan is shown in figure 2.2(a), the color scale shows the measured currents in nA. As expected the currents on the edges of the module are lower than in the center, which is due to the profile of the scanning source. The decrease in current around 90 cm and 170 cm is due to the wire locators. Also, a lot of spots with lower currents are visible in the center of the module, these are the results of previous ageing sessions[1].

Figure 2.2(b) shows a second scan of the module after the module has been aged for 190 hours. This is accomplished by placing a 2 mCi ^{90}Sr source above wire 32 at a position of 30 cm along the module at a high voltage of 1550 V. More details on the setup to invoke ageing in the modules can be found in section 2.4. The second scan looks nearly identical to the first one, except for the spot with lower currents around 45 cm.

To distinguish the lower currents due to the ageing test from the effects of earlier tests, the source profile and the wire locators, the ratio of both scans is taken. This is shown in figure 2.2(c), while a close-up of the ageing damage is shown in figure 2.2(d). In the pictures the gas flows from right to left. The color scale now indicates the value of the relative gain, where a value

[1]This module (number 121) has been used in numerous ageing tests over the past few years.

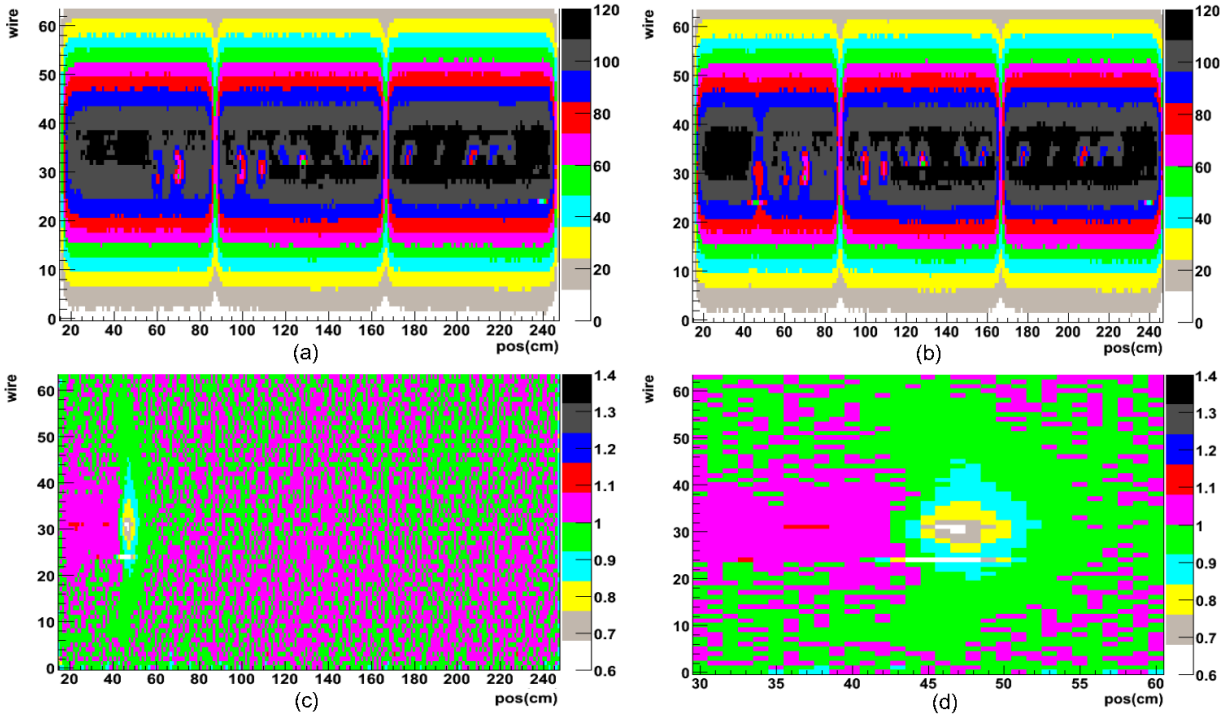

Figure 2.2: *(a) Scan of module 121B before an irradiation test with a 2 mCi ^{90}Sr source placed at 6 cm above wire 32 at 30 cm along the module. The color scale shows the measured current in nA and the gas flow is from right to left. (b) Scan of module 121B after the irradiation test of 190 hours. (c) Ratio of the scans, the color scale now shows the relative gain. (d) A zoom in on the location of the ageing damage. [Module 121B, 25/11/2009 - 03/12/2009]*

of 1 would indicate no gain loss[2].

The ageing in the Outer Tracker shows some strange characteristics [19], which can also be seen in figure 2.2(d):

⇒ Ageing only occurs upstream of the source. No ageing occurs downstream, presumably because of the production of ozone, which prevents the creation of the insulating layer.

⇒ The gain loss is not proportional to the source intensity, no ageing is visible directly below the source.

Figure 2.3 shows the gain loss versus intensity for several wires and confirms that no gain loss is visible at the position of highest intensity. Instead, a maximum in the gain loss is seen around an intensity of 0.05 nA/cm. Also, the amount of gain loss is not the same for all wires, although the source profile is symmetric. To create this plot, the intensity profile of the ^{90}Sr source has been used, for more details see section 2.4.

[2]Note that a 1% increase in air pressure already causes a decrease of the gain of about 5%, and has thus been corrected for in the normalization.

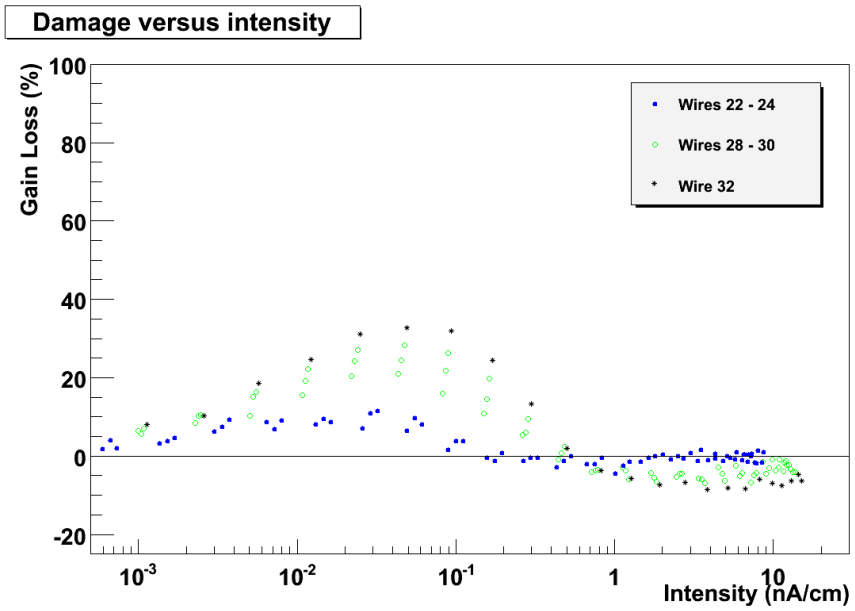

Figure 2.3: *The amount of gain loss versus the intensity of the source for multiple sets of wires.*

There are several ways to quantify the amount of ageing [3]. The minimum method takes the amount of ageing to be the maximum gain loss in some region. For example, the amount of ageing in figure 2.2(d) is approximately 35%. A downside of this method is that it only looks at the maximum gain loss and does not take the physical size of the aged spot into account. Besides this downside, it suits our purposes and will be used in the remainder of this thesis to quantify the ageing.

2.3 Overview of treatments

Since the ageing was only discovered after all the modules were constructed and installed in the LHCb experiment, it is not feasible to rebuild all of them. Instead, other ways to prevent and repair the gain loss of the detector have been devised and some of these have already been implemented in the experiment.

There are several ways to prevent the detector from ageing [20]:

⇒ Heating the module: this increases the outgassing rate of the glue.

⇒ Lowering the gas flow: this reduces the removal of ozone from the gas mixture and gives more prevention upstream.

⇒ Adding a few percent of oxygen to the gas mixture: this increases the formation of ozone, increasing the prevention downstream of the source.

As a result, the gas flow[3] of the modules in the experiment has been lowered from approx-

[3] A gas flow of 20 L/hour corresponds to one volume exchange per hour.

imately 20 L/hour to approximately 5 L/hour and the gas mixture has been changed from Ar/CO_2 70/30 to $Ar/CO_2/O_2$ 70/28.5/1.5 [21].

Besides these preventive measures, a method has been developed to remove the insulating layer once the detector suffers from irradiation damage. This method, called HV training, consists of increasing the high voltage applied to the module such, that the drift tubes enter the discharge regime and produce high dark currents. More specifically, the HV training implies a high voltage around 1900 V, inducing dark currents of about 10 μA per wire. This method has proven to repair damage from ageing, and even prevent future gain loss to some extent [22]. As noted before, the discharges do not necessarily occur at the location of the ageing, so that some gain loss might be difficult to repair with this method. Chapter 4 describes an upgrade of this method, where a source is used to cure the module at the desired location.

2.4 Radiation intensity

To invoke ageing in the modules two different setups are used. In the first setup, the 20 mCi ^{90}Sr source which is used for scanning the module is also used to invoke ageing. Typically the high voltage will be set to 1600 V during these ageing sessions. A picture of the setup is shown in figure 2.1(a). The disadvantage of this setup is that it does not create an intensity profile comparable to that of the LHC beam, as shown in figure 2.4.

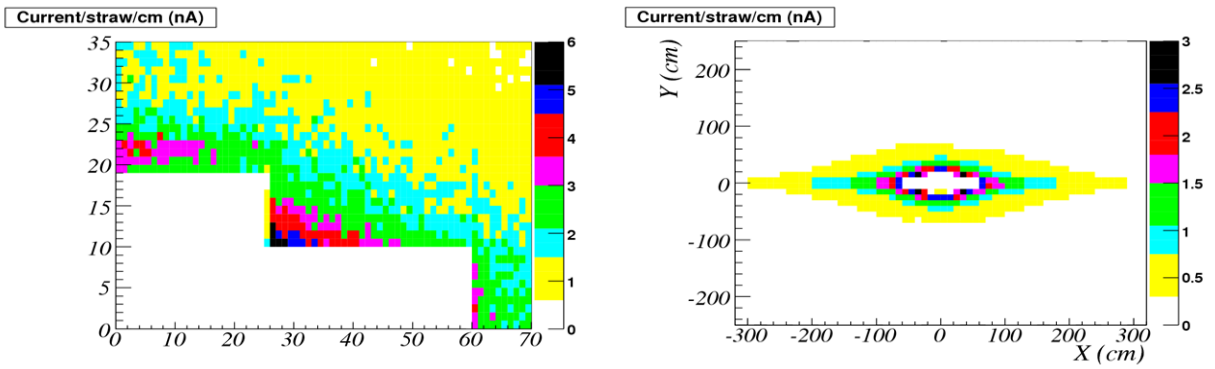

(a) (b)

Figure 2.4: *(a) Two dimensional intensity profile of the LHC beam in the OT. (b) Zoom in of the intenstity profile, the beam pipe and Inner Tracker are located in the white region at the lower left [23].*

To calculate the intensity profile of the source, the profile along the length of the module is needed. The source profile as shown in figure 2.1(b) only shows the current per wire, since the current meter measures the integrated current along each of the wires. The profile of the scanning source along the module has been measured to be Gaussian with a full width of 0.92 cm [3]. Furthermore, the profile of the source perpendicular to the wires is described rather well

with a double Gaussian[4], so the two dimensional intensity profile of the scanning source is given by:

$$I_{big}(x,y) = (A_1\, e^{x^2/\sigma_1^2} + A_2\, e^{x^2/\sigma_2^2})\, e^{y^2/0.46^2} \tag{2.1}$$

where x is the distance perpendicular to the wires, y is the distance along the wires and A_1, A_2, σ_1 and σ_2 are fit parameters.

Since the current meter integrates the currents along the wires, the source profile as measured by the current meter can be obtained by integrating equation 2.1 over y:

$$S_{big}(x) = \int_{-\infty}^{\infty} (A_1\, e^{x^2/\sigma_1^2} + A_2\, e^{x^2/\sigma_2^2})\, e^{y^2/0.46^2}\, dy = 0.46\sqrt{\pi}\,(A_1\, e^{x^2/\sigma_1^2} + A_2\, e^{x^2/\sigma_2^2}) \tag{2.2}$$

Figure 2.5(a) shows the measured source profile of the 20 mCi scanning source, fitted with equation 2.2. Using the values for the parameters as obtained from this fit gives the two dimensional intensity profile as shown in figure 2.5(b). It can be seen that the intensity profile of the scanning source is indeed quite different from that of the LHC beam.

To obtain a source which generates the same intensity profile as the LHC beam, the setup as shown in figure 2.6 will be used. A 2 mCi ^{90}Sr source is placed in a plexiglass cylinder with a radius of 15 cm at 6 cm above the module.

Since the 2 mCi source is not collimated like the scanning source, the intensity profile will be symmetric in x and y:

$$I_{small}(x,y) = A_1\, e^{(x^2+y^2)/\sigma_1^2} + A_2\, e^{(x^2+y^2)/\sigma_2^2} \tag{2.3}$$

and the measured current profile is given by integrating equation 2.3 over y:

$$S_{small}(x) = \sqrt{\pi}\, A_1\, \sigma_1\, e^{x^2/\sigma_1^2} + \sqrt{\pi}\, A_2\, \sigma_2\, e^{x^2/\sigma_2^2} \tag{2.4}$$

During the ageing sessions the high voltage will be set to 1500 V. This gives a current profile nearly identical to the one from the LHC beam, as can be seen from figures 2.5(c) and (d). The peak current in the LHCb experiment is about 6 nA/cm, while the peak current at 1500 V is about 7 nA/cm.

[4] A double Gaussian is needed instead of a single one, to fit the tails of the profile correctly.

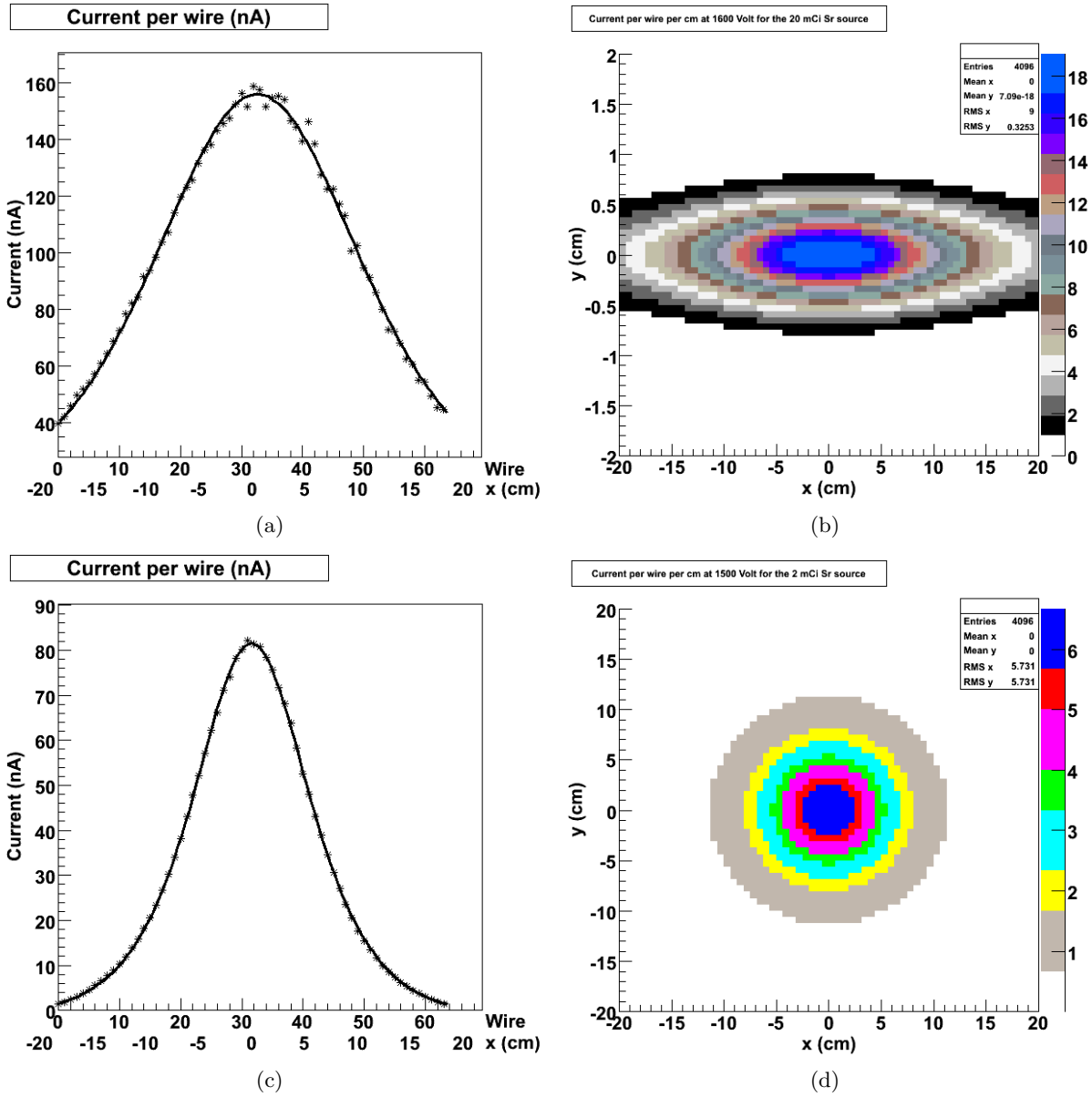

Figure 2.5: *(a) Measured source profile of the 20 mCi ^{90}Sr source at 1600 V. (b) Intensity profile of the scanning source at 1600 V. (c) Measured source profile of the 2 mCi ^{90}Sr source at 1500 V. (d) Intensity profile of the 2 mCi ^{90}Sr source at 1500 V.*

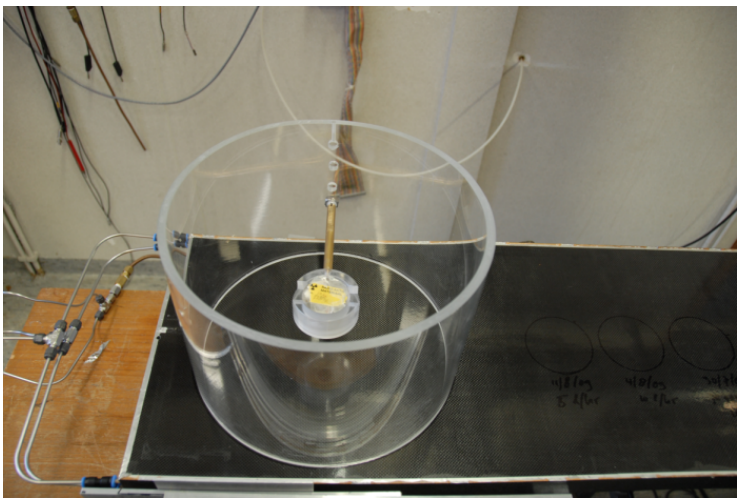

Figure 2.6: *Ageing setup used to create LHCb-like intensities.*

2.5 Glue

Finally, in this section it will be shown that indeed the plastifier is the main cause of the irradiation damage as described in the previous sections. To check the effect of the plastifier in the glue, an F module (dubbed *module 133*) was constructed using Araldite AY105-1 glue [24]. This glue is very similar to Araldite AY103-1, the only difference being that it does not contain the harmful plastifier di-isopropyl-naphthalene. Because of this, no strong ageing effects are expected under irradiation.

Table 2.1: *Details of the three ageing sessions conducted on module 133 constructed with Araldite AY105-1.*

Ageing session	Side	y (cm)	Total irradiation time (hour)
1	A	445	504
2	A	135	1060
3	B	135	984

To test this hypothesis, module 133 has been irradiated three times, as summarized in table 2.1. Irradiations are done on both sides of the module, called A and B, since only 64 of the total 128 straws in a module can be read out at a time with the current meter. To invoke ageing, the scanning source is used[5] with the high voltage set to 1600 V and a 70/30 Ar/CO_2 gas mixture flushing at 20 L/hour.

Figure 2.7 shows a scan of module 133 after different irradiation times for ageing session 1. Even after 504 hours of ageing, the maximum gain loss is only about 5%. This should be compared to a gain loss of about 40% in 20 – 200 hours as observed in standard modules constructed with

[5]The reason for this is a practical one. The setup with the 2 mCi ^{90}Sr source is located in a different place, so the scanning source is also used to create ageing in this case.

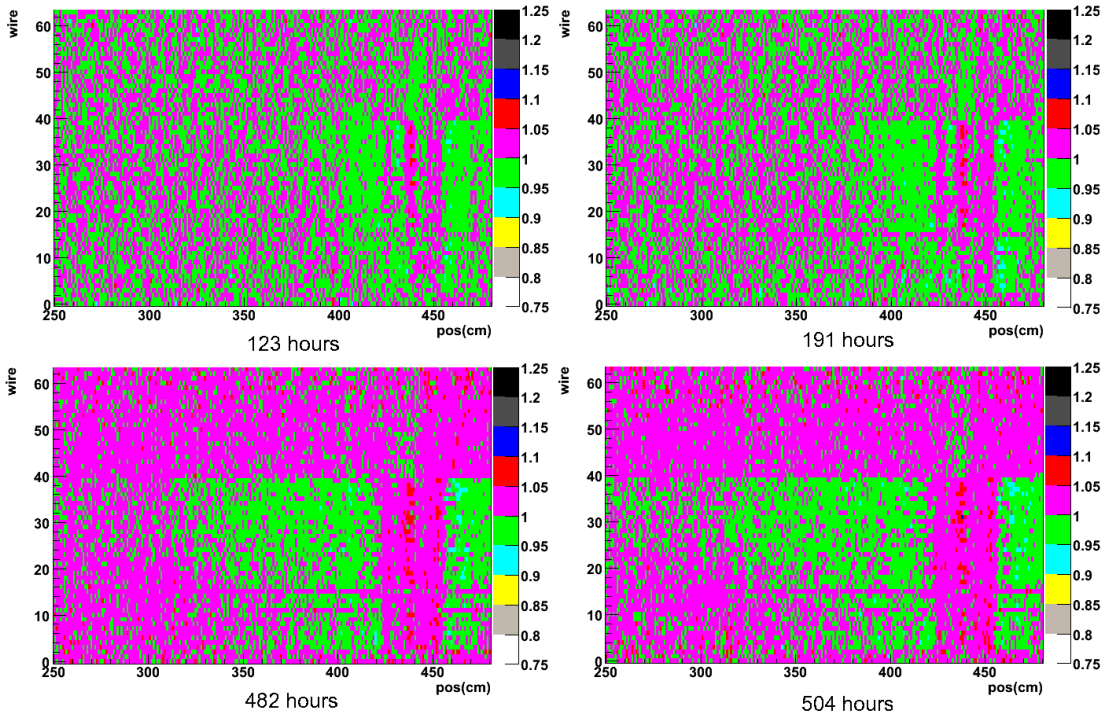

Figure 2.7: *Scan of module 133 after different irradiation times for ageing session 1: A side, scanning source at 445 cm. [Module 133A, 31/12/2009 – 21/01/2010]*

AY103-1. Interestingly, the gain loss is only observed in wires 1 to 40 and not in wires 41 to 62. An exception to this are the single wires 12 and 16, which do not show gain loss either. Also, no gain loss is observed directly below the source.

Because of the different amount of gain loss, presumably the observed gain loss is unrelated to our "normal" ageing and could be due to any component in the OT module. However, since only some wires show ageing effects, a difference in wire quality (which can differ between spools) could explain the effect.

The sharp transition around channel 40 could in principle also be caused by the straw material of the cathode. At construction, the lower and upper halves of the module are indepently supplied with straws. The anode wire on the other hand, is placed in the upper and lower half as one piece, before being separated in the middle of the module. This implies that if the strange pattern observed in figure 2.7 is due to the wires, it should also be visible when ageing the module in the lower half. Ageing session 2 is therefore conducted at 135 cm, the results are shown in figure 2.8.

In figure 2.8 the same pattern is visible; wires 1 to 40 show a maximum gain loss of about 5%, while wires 41 to 62 do not show any gain loss even after 1060 hours of irradiation. Also, wires 12 and 16 do not show ageing effects, just as before. This seems to point to a difference in wire quality as the reason that some wires show gain loss, while others do not.

As a final test, the other side of module 133 has been irradiated for a total of 984 hours. The results of this irradiation are shown in figure 2.9 and do not show the same wire to wire

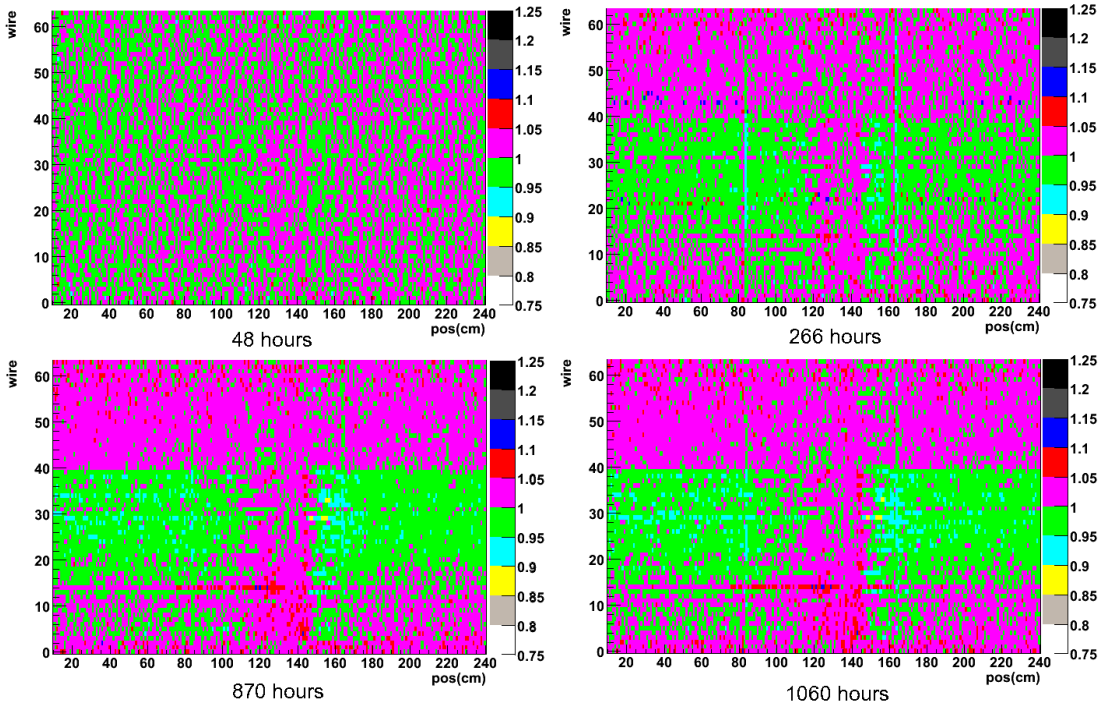

Figure 2.8: *Scan of module 133 after different irradiation times for ageing session 2: A side, scanning source at 135 cm. [Module 133A, 25/01/2010 – 10/03/2010]*

difference as observed on the A side. However, some gain loss (about 5%) is visible downstream of the source, which is placed at 135 cm. This has been observed earlier, during irradiation of a module constructed with Trabond glue[6] [25, 26], but the reason for this gain loss is not understood.

Because the gain loss is rather small and the irradiation time is large, this effect has not been observed during earlier ageing tests. However, because of these reasons, it does not hinder detector operation either. The Outer Tracker detector is designed to withstand an irradiation dose of about 2 C/cm/wire [17], while it will receive a yearly dose of about 0.06 C/cm/wire at the region of highest intensity[7]. Taking the intensity of the source to be on average 50 nA/wire/cm (see figure 2.5(b)) and the irradiation time to be about 1000 hours, shows that module 133 has received an irradiation dose of about 0.18 C/cm/wire during ageing sessions 2 and 3. This is comparable to 3 years of OT operation, which confirms that the observed gain loss does not pose a problem.

[6]Trabond is another type of glue, different from Araldite AY103-1 and AY105-1.

[7]Looking at figure 2.4(b) it can be seen that the highest intensity is about 6 nA/cm/wire, assuming that the LHC runs about one third of a year gives the stated value for the yearly dose.

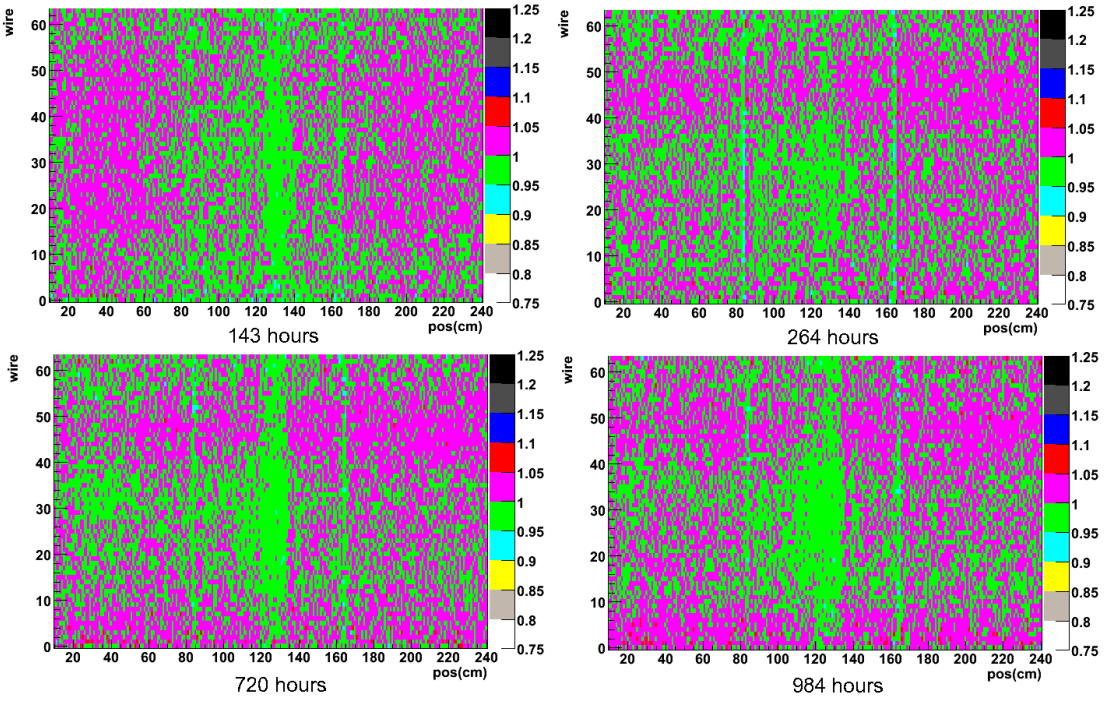

Figure 2.9: *Scan of module 133 after different irradiation times for ageing session 3: B side, scanning source at 135 cm. [Module 133B, 16/03/2010 – 17/05/2010]*

2.6 Summary

To detect ageing in an OT module, the currents induced by scanning the module with a 20 mCi ^{90}Sr source are measured. By dividing a scan after an ageing session by a scan done before, the relative gain can be calculated. The amount of ageing in a module is taken to be the maximum relative gain loss.

Two setups are used to invoke ageing in the modules. In the first setup, the 20 mCi ^{90}Sr scanning source is also used to age the module. A second ageing setup has been created using a 2 mCi ^{90}Sr source, which gives an intensity profile comparable to the LHC beam at a high voltage of 1500 V.

The effect of the plastifier in the Araldite AY103-1 glue, which is the cause of the ageing problem of the OT, has been examined by constructing a new module (133) with Araldite AY105-1. AY105-1 is identical to AY103-1, the only difference being that it does not contain the harmful plastifier. It has been verified that this module does not exhibit the normal ageing problem. Even after an integrated dose of 0.18 C/cm/wire, which corresponds to about 3 years of OT operation, the maximum gain loss is only about 5%, which does not hinder detector operation.

Chapter 3

Outer Tracker simulation

Adding a small amount of oxygen to the gas mixture of the Outer Tracker has been shown to have a benificial effect on the ageing [27], so 1.5 % oxygen has been added while slightly lowering the CO_2 percentage. However, since oxygen is an electronegative gas, it can capture the drifting primary electrons, thereby effectively lowering the signal response or even losing efficiency. Earlier studies [4] did not show any decrease in the gain when adding oxygen. The reason for this is that these simulations only looked at electron multiplication in the avalanche region. This chapter describes the results of simulations taking electron capture in the complete drift region into account.

To simulate the Outer Tracker, the GARFIELD version 9 and MAGBOLTZ version 7.07 programs will be used, which will be described in more detail in section 3.1. Both the effect on the signal loss and on the efficiency, by adding oxygen to the gas mixture, will be simulated.

Section 3.2 describes the general details of the OT simulation and the determination of the survival probability of a single cluster of electrons. The single cluster survival probability will be used to calculate the effect on the efficiency in section 3.3.

In section 3.4 the effect on the signal loss by adding oxygen to the gas mixture will be described. A distinction will be made between the effect on a ^{90}Sr source and a ^{55}Fe source, since earlier results [4] have indicated that both sources give a different result for the signal loss due to the addition of oxygen. The simulated results will be compared to experimental results for both sources to see if this difference can be explained.

In the simulations done in this chapter, the small magnetic field which is present in the Outer Tracker is not taken into account. In section 3.5 the effect of the magnetic field on the drift time of the electrons is simulated to verify that this assumption is valid.

3.1 Programs used for the simulation

GARFIELD is a program for the detailed simulation of two- and three-dimensional drift chambers of almost any shape and wire configuration [28]. The built-in *tube* geometry, which consists of an anode wire enclosed by a cathode tube, will be used to simulate the Outer Tracker straws. As input the radius, length and voltage of the tube, the diameter, tension, voltage and position of the wire and the properties of the gas mixture are needed as input for GARFIELD.

The gas properties can be calculated using GARFIELD itself, but using the interface to the MAGBOLTZ program [29,30] greatly improves the accuracy of the calculation. MAGBOLTZ numerically solves the Boltzmann equation for electrons in an electric field. As input the pressure, temperature, gas mixture and drift cell layout have to be given. MAGBOLTZ will then calculate the drift velocity, the longitudinal and transverse diffusion coefficients, the Townsend and attachment coefficients as well as the excitation and ionisation rates for the various gas molecules.

3.2 Simulating the Outer Tracker

In this section the general details of the OT simulation will be described for the passing of an electron through the Outer Tracker. Also, the determination of the single cluster survival probability will be described. The simulations will be done for different percentages of oxygen in the counting gas, the percentage of argon remains 70%.

As described in the introduction, an electron traversing the drift chamber will have several ionizing collisions with the gas molecules, giving rise to the primary ionizations. Together with the secondary ionizations they form the total ionization. The number of ionizations for the individual gases used in the Outer Tracker are given in table 3.1. The primary and total number of electron-ion pairs per unit length for gas mixtures can be calculated assuming a simple composition law:

$$n_{t,mix} = \sum_{i=1}^{n} f_i \, n_{t,i} \tag{3.1}$$

where f_i is the fraction of gas i in the mixture. The mean distance between the clusters, λ, is found by inverting equation 3.1:

$$\lambda = \frac{1}{n_{p,mix}} \tag{3.2}$$

and is roughly equal to 327 μm for $Ar/CO_2/O_2$ 70/28.5/1.5. However, the effective ionization length as measured in the OT is larger. For example, some clusters can be missed if the charge is not above the minimum threshold as set in the ASDBLR. A more realistic value for λ is 850 μm, as described in [31]. Simulations will be done for both values. Note that the effective ionization length affects the inefficiency at the edges of the straw. The probability to create zero clusters along the particles path through the straw when μ are expected is given by a Poisson distribution:

$$P(0, \mu) = e^{-\mu} \tag{3.3}$$

with μ given by:

$$\mu = L/\lambda = 2\sqrt{R^2 - r^2}/\lambda \tag{3.4}$$

with L the length of the track in the straw, r the distance of closest approach of the track and R the radius of the cell as defined in figure 1.2.

The passing of an electron can be simulated by letting GARFIELD create a track with a number of clusters. The position and number of these clusters will be randomly generated by the program. As input GARFIELD needs the mean number of clusters (which is equal to the

Table 3.1: *Primary and total number of created electron-ion pairs and the mean number of electrons per cluster for the gases used in the OT simulation and the gas mixture used in the experiment [12].*

Gas	n_p (pairs/cm)	n_t (pairs/cm)	electrons/cluster
Ar	29.4	94	3.2
CO_2	34	91	2.7
O_2	22	73	3.3
$Ar/CO_2/O_2$ **70/28.5/1.5**	30.6	92.8	3.1

number of primary ionizations) and a cluster size distribution function. The distribution can be approximated by a simple power law [32]. Since the main part of the gas mixture is argon (and the differences in distribution between argon and oxygen are small), the distribution function for argon will be a good approximation for all gas mixtures used. It can be seen from table 3.1 that a cluster in argon contains about 3.2 electrons, which is reproduced by using the cluster function:

$$P(n) = \frac{1}{\zeta(2.25)\, n^{2.25}} \tag{3.5}$$

where P(n) is the probability that a cluster has size n (with n an integer) and ζ the Riemann zeta function, taking care of the normalization ($\zeta(2.25) \approx 1.46$).

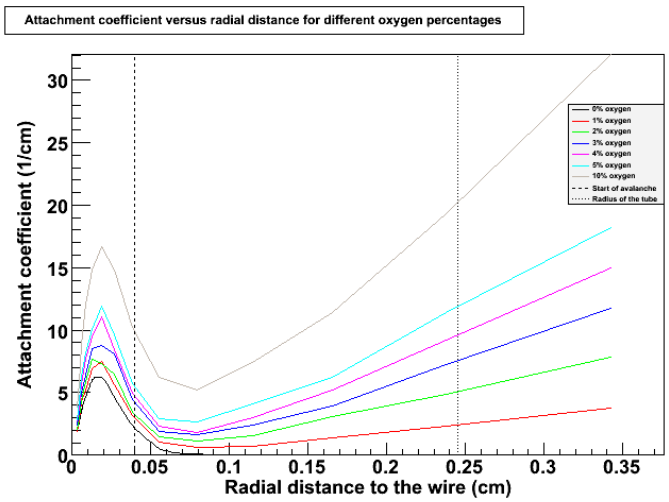

Figure 3.1: *Attachment versus radial distance for the different gas mixtures used in the simulation.*

3.2.1 Single cluster survival probability

In the next sections, the total signal loss and the probability to miss a hit due to electron capture by the oxygen will be estimated. First, the single cluster survival probability will be defined and quantified. To check if a cluster on the track survives, every electron in the cluster is drifted

towards the anode wire. The electrons are drifted one after the other, since GARFIELD can not take interactions between the electrons in a cluster into account. Outside of the avalanche area, the electron can be captured by an electronegative molecule (either O_2 or CO_2), as quantified by the attachment coefficient, see figure 3.1. Once the electron reaches the avalanche area, electron attachment can be neglected and the electron will reach the wire. A cluster is said to have survived if one or more of the electrons of the cluster are detected. The single cluster survival probability is then given by the number of clusters that survived divided by the total number of clusters averaged over many tracks. The single cluster survival probability will be used in section 3.3 to calculate the inefficiency, i.e. the probability of not detecting a passing electron. Figure 3.2 shows an example track, where the stars mark the attachment of an electron.

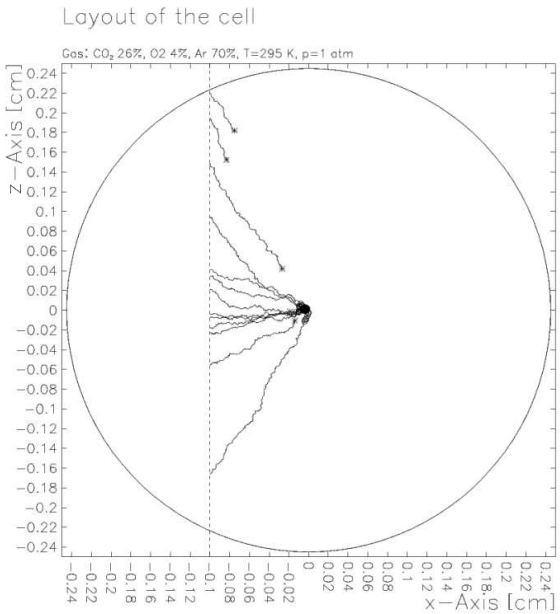

Figure 3.2: *Example of a track through an Outer Tracker drift cell. A number of clusters are created on the track and the electrons are drifted to the anode wire.*

The single cluster survival probability for different fractions of O_2 in the gas mixture is quantified as follows. The radial distance between the anode wire and the cathode tube (distances between 0.00125 cm and 0.245 cm) is equally divided into 25 points. At each point 500 vertical tracks are created, for which the survival probability of the clusters is calculated. This gives the results as shown in figure 3.3, where the dotted line marks the position of the cathode tube. The graphs have been fitted with two straight lines: one in the avalanche region and one outside the avalanche region:

$$p(r) = \begin{cases} 1 - a_1 \times r & \text{if } r \leq 0.04 \text{ cm} \\ b_0 - b_1 \times r & \text{if } r > 0.04 \text{ cm} \end{cases} \tag{3.6}$$

where p(r) is the single cluster survival probability as a function of radial distance r of the cluster to the wire and a and b are fit parameters.

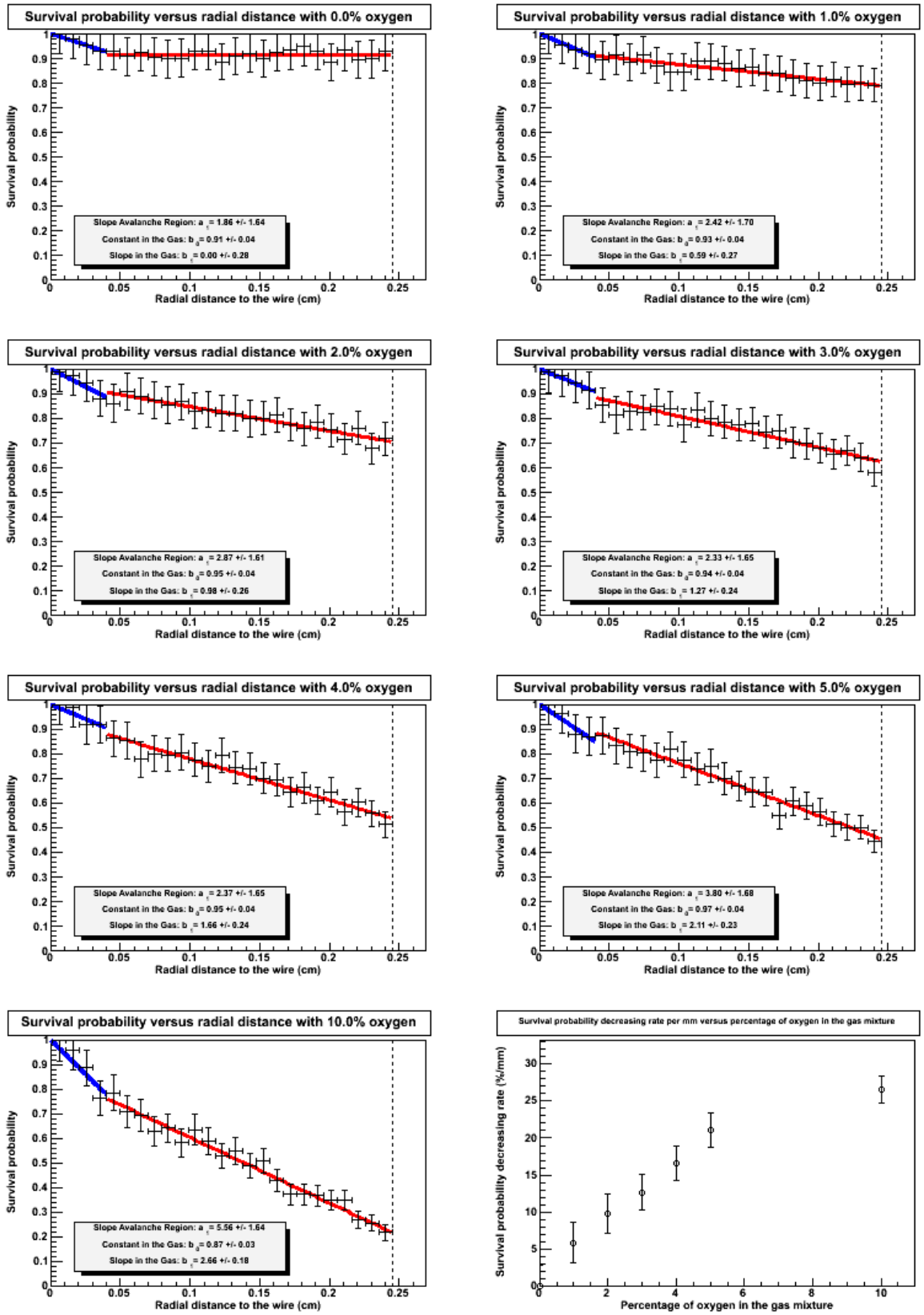

Figure 3.3: *Single cluster survival probability versus radial distance of the cluster to the wire for the different gas mixtures used. The graphs are fitted with two straight lines, the lower right graph summarizes these results.*

The slopes of the fits outside the avalanche region are summarized in the lower right graph of figure 3.3 and give the decrease in survival probability per mm as a function of the amount of O_2 in the gas mixture. As expected, this decrease is bigger for higher oxygen percentages, since more oxygen leads to more attachment.

3.3 Effect on efficiency: probability of missing a track

The values obtained from the fits of the single cluster survival probability will be used to calculate the probability of not detecting a passing electron. This happens if none of the clusters on the track survives and is given by:

$$P_{miss}(r) = \prod_{i=1}^{N} 1 - p(r_i) \tag{3.7}$$

where $P_{miss}(r)$ is the probability of not detecting a passing electron, N is the number of clusters on the track, r_i is the radial distance of the i-th cluster to the anode wire and $p(r_i)$ is the single cluster survival probability obtained from figure 3.3.

The radial distance between anode wire and cathode tube is equally divided into 50 points and at each point 500 vertical tracks are created. The radial distance to the wire is measured from the middle of the track (i.e. the distance of closest approach of the track). Figure 3.4 gives the results of the simulation for different oxygen percentages in the mixture where λ is calculated according to equation 3.2. Figure 3.5 shows the results for $\lambda = 850$ μm. To guide the eye, a reference line has been drawn at an inefficiency of 20 percent. The lower right graph in figures 3.4 and 3.5 shows the average inefficiency for the different oxygen percentages, assuming that the tracks will be distributed equally over the radial distance.

It can be seen from figure 3.4 that the probability to miss an electron (using the theoretical values for λ) is rather small for small radial distances, even for an oxygen percentage of 10%. The probability of missing a track quickly increases for an increasing distance to the wire, due to two effects. First of all, the electrons have to traverse a greater distance, increasing the chance that they will be attached. Secondly, since the drift area is circular, tracks on the outside of the tube will have less clusters, increasing the probability of not detecting the passing electron. From the lower right graph in figure 3.4, which has been fitted with a parabola to guide the eye, it can be seen that adding 1.5% oxygen to the gas mixture decreases on average the efficiency to detect a traversing particle by only about 0.7%.

With a more realistic value, $\lambda = 850$ μm, the addition of 1.5% oxygen to the gasmixture gives on average a chance of about 5.5% to miss a passing electron, which is about 1.5% more inefficient compared to no oxygen in the gas mixture. Adding more than 5% O_2 is not advisable, since more than 11% of the passing electrons will not be detected for that oxygen percentage.

Since the Outer Tracker modules contain two staggered layers of straw tubes, the average track loss is not so high. If a particle traverses one of the straws near the outside of the tube, it will traverse the next straw more in the centre of the tube.

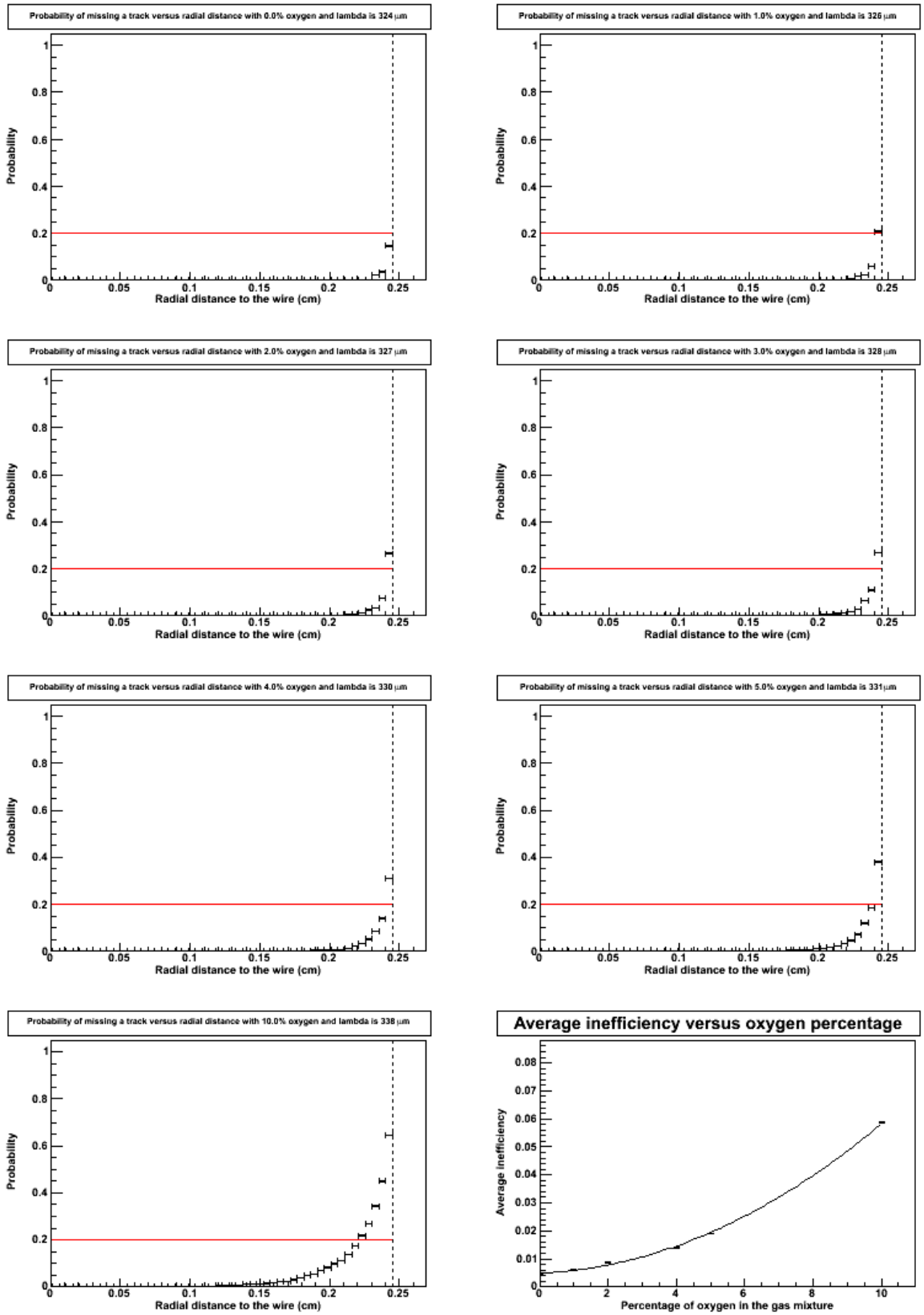

Figure 3.4: *Probability of not detecting an electron versus radial distance for the different gas mixtures used, λ is calculated using equation 3.2. The lower right graph shows the average inefficiency versus the oxygen percentage.*

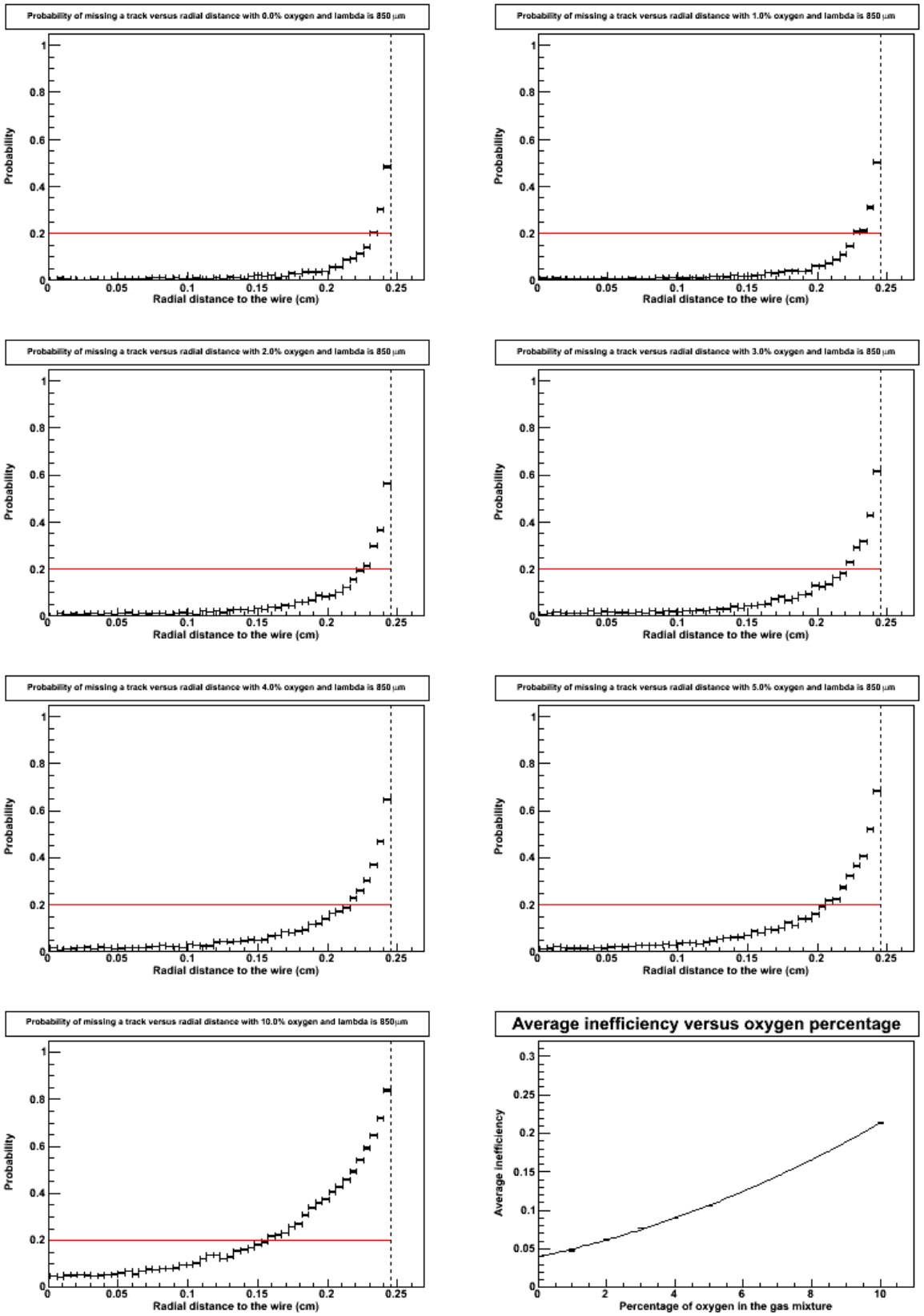

Figure 3.5: *Probability of not detecting an electron versus radial distance for the different gas mixtures used, $\lambda = 850\ \mu m$. The lower right graph shows the average inefficiency versus the oxygen percentage.*

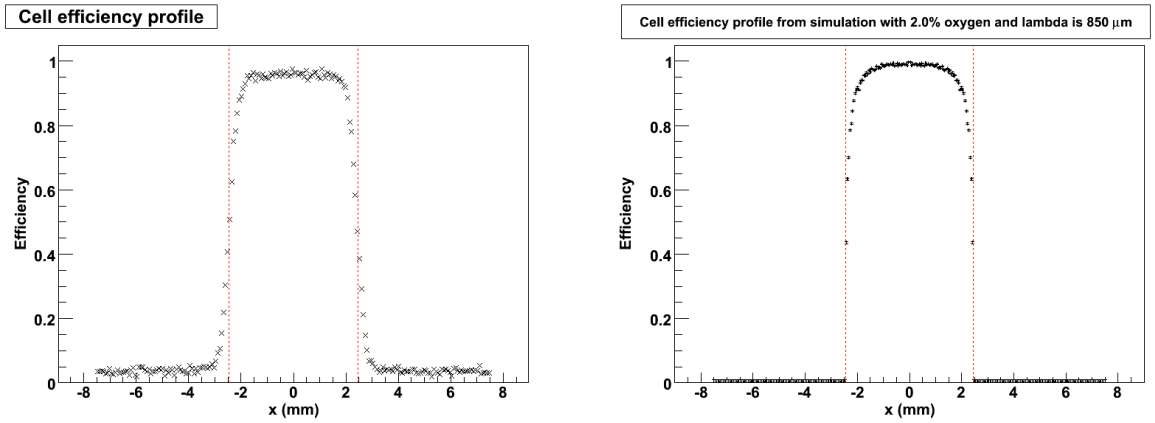

(a) (b)

Figure 3.6: *(a) Cell efficiency profile obtained from the OT, the red lines mark the radius of the drift cell. (b) Cell efficiency profile obtained from simulation.*

It is interesting to compare the simulated results with results obtained from the Outer Tracker itself. Figure 3.6(a) shows the cell efficiency profile as obtained from experiment [33]. It has been obtained by measuring the percentage of the tracks that is measured by the straw tube as a function of the x position of the track. Figure 3.6(b) shows the cell efficiency profile obtained from simulation for an oxygen percentage of 2% and $\lambda = 850$ μm. It has been created by inverting the graph with the probability of missing a track from figure 3.4 and using x as variable instead of the radial distance.

The results from experiment and simulation are in good agreement, except for values of x bigger than 2.45 mm, which is outside of the drift cell. In the simulation, the chance of detecting a particle which misses the straw tube is zero, which is not the case for the real OT drift cells. The reason for this is cross-talk, where a hit in a straw also induces a signal in the neighbouring straw and the position resolution.

3.4 Simulation of the effect of O_2 on the signal height

Apart from increasing the probability of not detecting an electron, adding oxygen to the counting gas also decreases the signal, since less clusters reach the anode wire. The signal loss relative to 0% oxygen can be calculated analogously to the calculation of the single cluster survival probability. This will in section 3.4.1 be done for electrons emitted by a ^{90}Sr source and in section 3.4.2 for photons emitted by a ^{55}Fe source. The results of these simulations are compared to experimental results in section 3.4.3.

3.4.1 Signal loss for ^{90}Sr

The fraction of the electrons on a track that reaches the wire will be used to determine the relative signal amplitude[1]. The radial distance between anode and cathode is equally divided into 30 points and at each point 100 (vertical) tracks are created. The results for different percentages of oxygen are summarized in figure 3.7.

The upper left graph in figure 3.7 shows that about 14% of the clusers do not reach the wire, even for a gas mixture without O_2. This can be explained by noting that CO_2 is also an electronegative gas (although less so than oxygen), leading to some attachment. A reference line at this percentage is also shown in the other graphs in figure 3.7. The average signal loss is indicated by the horizontal line in the graphs. The average signal loss relative to 0% oxygen is plotted against the oxygen percentage in the lower right graph of figure 3.7 and has been fitted with a parabola to guide the eye. From this it can be seen that adding a few percent oxygen reduces the signal quite strongly. By adding 1.5% oxygen, the average signal decreases by approximately 16%.

3.4.2 Signal loss for ^{55}Fe

The major difference between the ^{90}Sr and the ^{55}Fe source, is that the first emits electrons of energies up to 2 MeV, while the latter emits monochromatic photons with an energy of 5.9 keV. One photon will ionize one argon atom by means of the photo-electric effect. The liberated electron will then create a single cluster of primary electrons. The simulations will again be done for different percentages of oxygen in the counting gas, the percentage of argon remains 70%.

A photon can be simulated in GARFIELD by creating a single cluster of N primary electrons, where N is distributed according to a Gaussian distribution with mean and variance given by [34]:

$$N_{mean} = \frac{5900\,[\text{eV}]}{W} \tag{3.8}$$

$$\sigma^2 = \frac{F\,N_{mean}}{W} \tag{3.9}$$

where W is the mean energy per ion pair in eV and F is the Fano factor. For a 70/30 mixture of Ar/CO_2, W is about 28.4 eV and F is 0.21, giving a mean of about 207 electrons and a variance

[1]The simulations are done for the theoretical value of λ. Of course, the same results are obtained if the results for $\lambda = 850$ μm would be used, because the drift properties do not depend on the cluster formation.

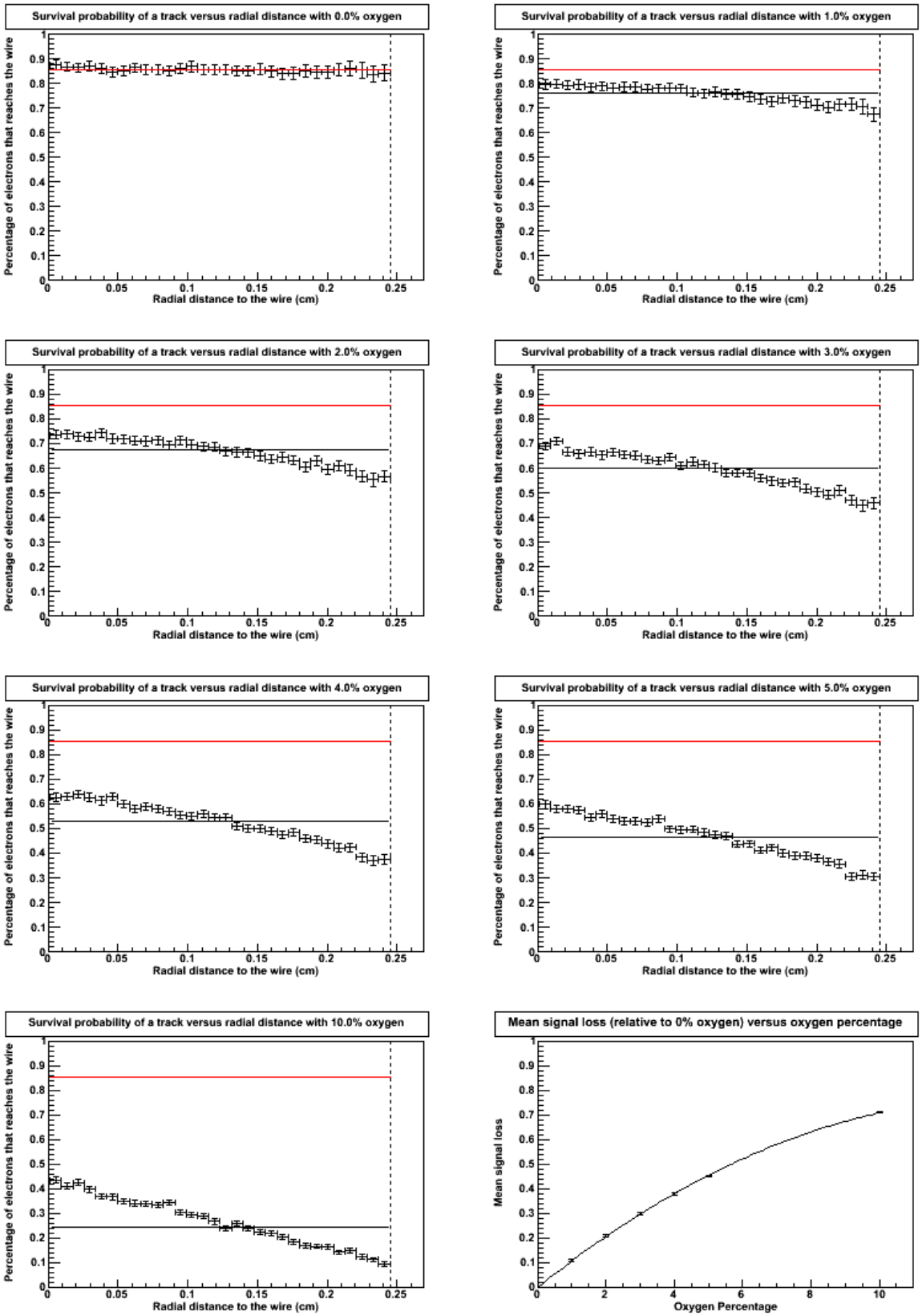

Figure 3.7: *Percentage of electrons on the track that survives versus radial distance for the different gas mixtures used. The lower right graph shows the mean signal loss relative to 0% oxygen versus oxygen percentage.*

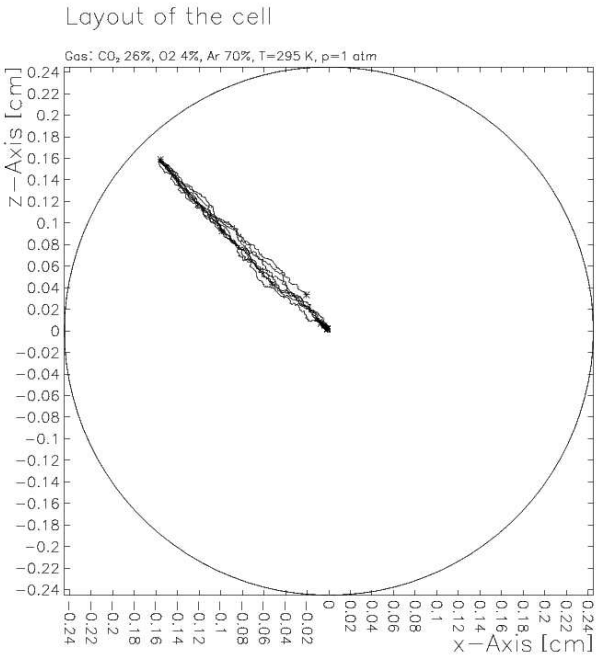

Figure 3.8: *Example of a photon in the Outer Tracker. A single cluster is created and the electrons are drifted to the anode wire.*

of 44. Replacing a fraction of the CO_2 by O_2 does not change the values of W or F significantly, so this distribution will be a good approximation for all used gas mixtures.

The signal loss calculation is performed analogously to the one for the ^{90}Sr source. In this case, a single cluster is created at a random position in the tube and all the electrons in the cluster are drifted to the anode wire one after the other, an example is shown in figure 3.8. In the figure only every 20th electron is plotted for clarity. For each gasmixture 50 clusters are generated. The results are shown in figure 3.9.

3.4.3 Comparison with experiment

The relative signal loss due to the addition of oxygen to the gas mixture can be compared to the signal loss as measured by experiment [4].

Table 3.2: *Experimental and theoretical values for the mean relative signal loss for several oxygen percentages for both the ^{90}Sr source and the ^{55}Fe source.*

O_2 percentage	Relative signal loss ^{90}Sr		Relative signal loss ^{55}Fe	
	From simulation	From experiment	From simulation	From experiment
2.5	0.26	0.20	0.26	0.10
4.5	0.43	0.45	0.43	0.28

Figure 3.9 shows the results for both the ^{90}Sr and ^{55}Fe sources and the experimental results

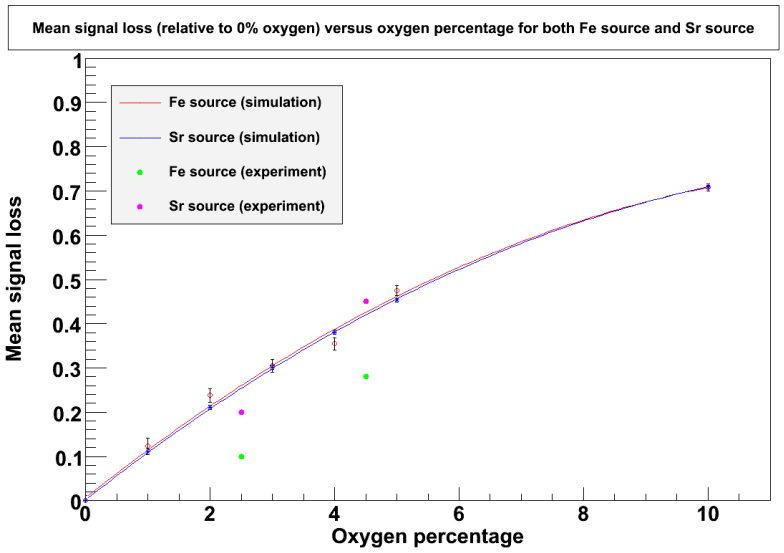

Figure 3.9: *Mean signal loss versus oxygen percentage for the both the ^{90}Sr and ^{55}Fe sources. The values from experiment are also shown.*

as measured in [4] for comparison. Both graphs have been fitted with a parabola to guide the eye. The results are summarized in table 3.2, the simulated results are obtained by interpolation.

The experimental and simulated results are in good agreement for the ^{90}Sr source, although the experimental signal loss at 2.5% O_2 is slightly lower than what is to be expected from simulation. The simulated signal loss for the ^{55}Fe source is identical to that of the ^{90}Sr source and is too high when compared to the experimental results. This can be explained by the fact that the electrons are drifted to the wire separately in the simulation, while in reality they all drift at the same time. In the case of the ^{55}Fe source there are so many primary electrons, that it is possible that all oxygen molecules on the drift path have already attached electrons and the remainder of the electrons simply reaches the wire. This idea is fortified by noting that the difference between simulation and experiment is smaller for higher oxygen percentages. In the simulation, this effect can not be taken into account (since the electrons are drifted one after the other), which might lead to an overestimation of the signal loss.

By adding 1.5% oxygen to the gas mixture, the average signal decreases by approximately 16% for both the detection of photons and electrons in the Outer Tracker.

3.5 Effect of the magnetic field on the drift time

In the signal loss simulations done in this chapter, the small magnetic field which is present in the Outer Tracker is not taken into account. In this section the effect of this field on the drift time is examined. If both an electric and a magnetic field are applied, the drift velocity is given by the Langevin equation [35]:

$$\mathbf{v}_d = \frac{\mu}{1 + (\mu B)^2} \left(\mathbf{E} + \mu \, \mathbf{E} \times \mathbf{B} + \mu^2 \, \mathbf{B} \, (\mathbf{E} \cdot \mathbf{B}) \right) \tag{3.10}$$

where μ is the mobility of the drifting particles (which is negative for electrons), **E** is the electric field vector, **B** is the magnetic field vector and B is the absolute value of the magnetic field vector.

In the OT, the magnetic field is oriented along the straw (the y-direction in figure 1.1), making it perpendicular to the electric field which is oriented in the r-direction. Equation 3.10 then simplifies to:

$$\mathbf{v}_d = \frac{\mu E}{1 + (\mu B)^2} \left(\hat{r} + \mu B \, \hat{\phi} \right) \tag{3.11}$$

where $\hat{r}$ is the unit vector in the r-direction and $\hat{\phi}$ the unit vector in the ϕ-direction.

From equation 3.11 it can be seen that the drift velocity is no longer parallel to the direction of the electric field. This results in a slightly curved drift path instead of a straight path, as can be seen in figure 3.10, where the drift path of several electrons is shown in a magnetic field of 2 Tesla.

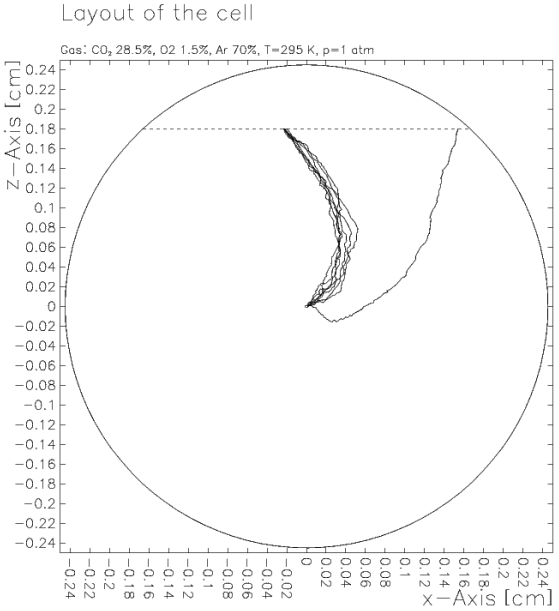

Figure 3.10: *Example of the drift of electrons from a particle track for a magnetic field of 2 Tesla.*

Because of the longer drift path and the smaller drift velocity when a magnetic field is present, the drift time of the electrons will also increase. From equation 3.11 it can already be seen that this effect will be larger for larger values of the magnetic field. To simulate this effect, the drift area is equally divided into 1000 points and at each point a track is created. For every electron in the clusters on the track, the drift time and the distance to the anode wire are calculated.

The Outer Tracker consists of three stations (labeled T1, T2 and T3) and the size of the magnetic field varies from station to station. Figure 3.11 shows the size of the magnetic field as a function of the distance from the collision point. From the figure, the size of the magnetic field at each OT station can be approximated. Simulations will be done for the magnetic field sizes as summarized in table 3.3.

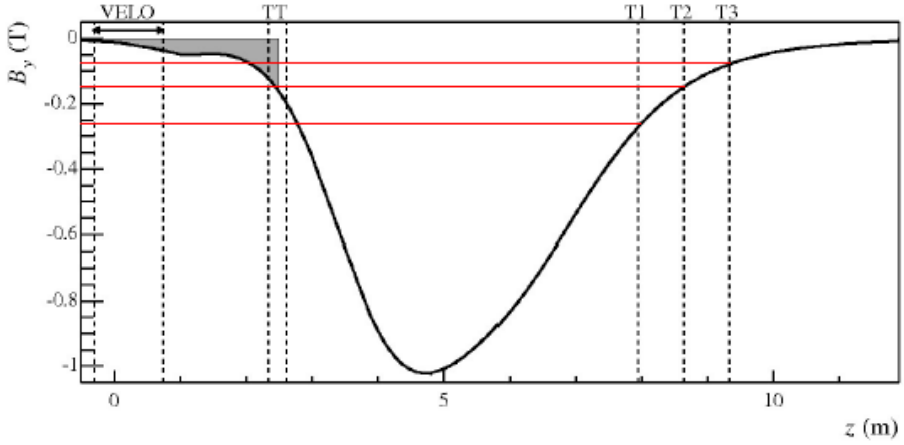

Figure 3.11: *Size of the magnetic field as a function of distance to the interaction point. The size of the field is shown at different sub-detectors [10].*

Table 3.3: *The magnetic field sizes used in the simulation.*

Magnetic field size (T)	Comment
0	To check the drift times when no magnetic field is present
0.08	Size of the field at T3
0.15	Size of the field at T2
0.26	Size of the field at T1
2	Large value to better see the effect of the magnetic field

Figure 3.12(a) shows the x-t relation for the magnetic fields under consideration. As expected, the drift time is larger for a larger magnetic field. It can also be seen that the difference in drift time between the OT stations is very small. The drift time is only seriously affected by the magnetic field for values much greater than those in the OT.

To see the effect in more detail the maximum drift time is calculated for each magnetic field. This is obtained by fitting the x-t relation with a parabola and taking the value at x = 0.245 cm (i.e. the outer edge of the drift area). The maximum drift time is plotted versus magnetic field in figure 3.12(b), where the value at 2 Tesla is omitted for clarity.

From figure 3.12(b) it can be seen that the difference in drift time between OT stations 1 and 3 is about 0.2 ns. The time resolution of the Outer Tracker is approximately 0.4 ns [36], showing that the effect of the magnetic field is negligible. Also, the length of the drift path increases only by about 0.7%, so the effect of the magnetic field on the signal loss is also negligible.

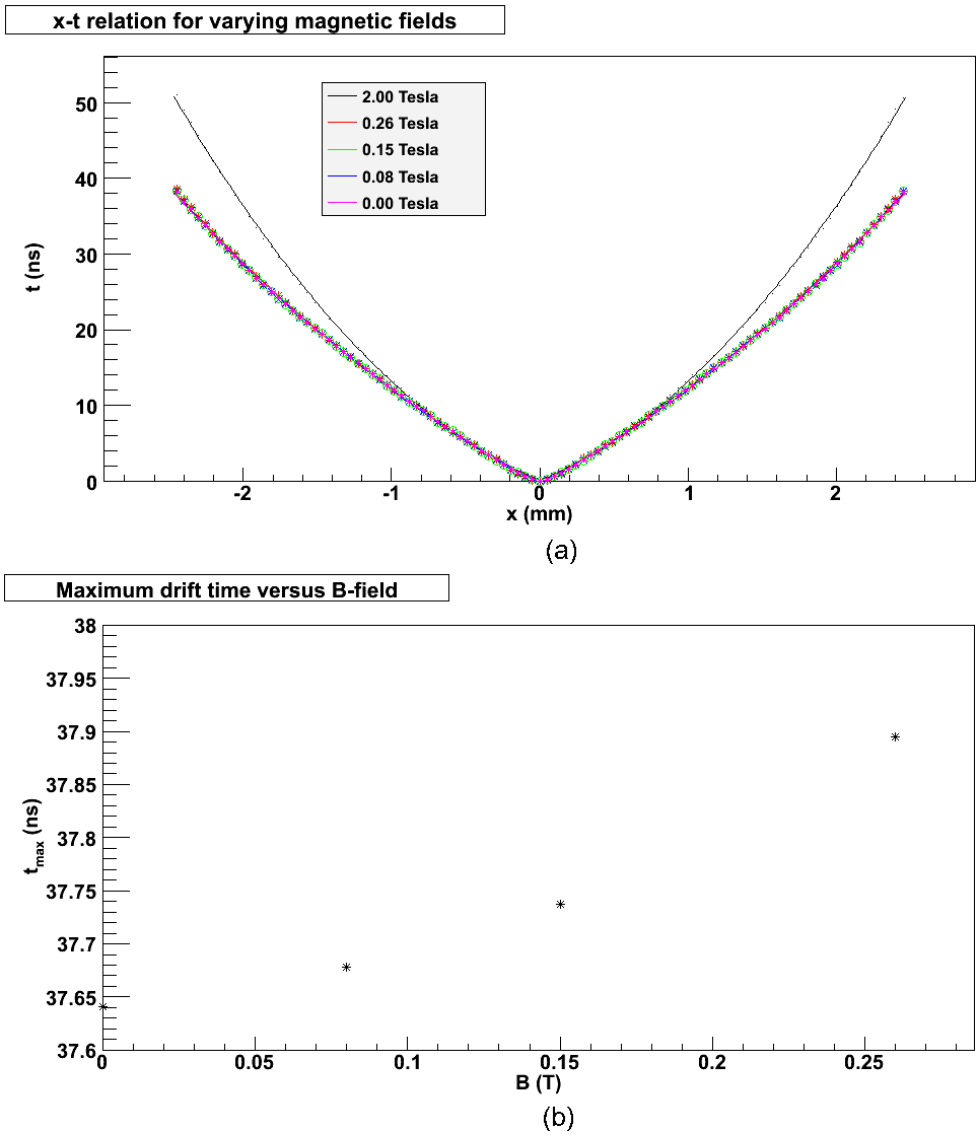

Figure 3.12: *(a) x-t relation for the different magnetic fields used in the simulation. (b) Maximum drift time of electrons versus magnetic field.*

3.6 Summary

The signal loss due to the addition of oxygen to the Outer Tracker gas mixture has been simulated. Simulations have been done for the effect on minimum ionizing particles (i.e. electrons emitted by the ^{90}Sr source) and for photons (emitted by the ^{55}Fe source). In both cases the addition of a few percent oxygen reduces the signal, but this does not hinder the operation of the Outer Tracker. The addition of 1.5% oxygen decreases the signal by about 16% for the detection of both electrons and photons.

Besides reducing the signal, adding oxygen also increases the chance of not detecting a passing particle, which happens if all drifting electrons are attached. For minimum ionizing particles this effect is important, especially for tracks near the edge of the drift area. For an oxygen percentage of 1.5, roughly 1% of the minimum ionizing particles are not detected for the theoretical value of λ. Using the more realistic value of 850 μm for λ shows that on average 5.5% of the passing particles will not be detected, which is 1.5% worse compared to no oxygen. The inefficiency is dominated by tracks near the edge of the drift area.

When comparing the simulated signal loss to the experimental values found for the Outer Tracker, it can be seen that the simulated signal loss at 2.5% oxygen is slightly too high compared to experiment, but the results are overall in reasonable agreement. The simulated signal loss for the ^{55}Fe source is too high compared to experiment. This is probably because the electrons are drifted to the wire separately in the simulation, which does not happen in reality. In the case of the ^{55}Fe source there are so many primary electrons, that it is possible that all oxygen molecules on the drift path have already attached electrons and the remainder of the electrons simply reach the wire. When the electrons are drifted separately, this saturation effect is not taken into account, thus overestimating the signal loss.

In the simulations done in this chapter, the small magnetic field which is present in the Outer Tracker is not taken into account. Applying a magnetic field increases the drift time of the electrons, since the drift path then becomes slightly curved, instead of a straight line. From simulation, the difference of maximum drift time between OT stations 1 and 3 is about 0.2 ns. Since the time resolution of the Outer Tracker is approximately 0.4 ns, the effect of the magnetic field on the drift properties is negligible.

Chapter 4

Curing with a source

As described in chapter 2, several solutions to remove or reduce ageing exist: flushing, heating and HV training. Both heating and flushing reduce the ageing rate, and therefore the Outer Tracker modules started being flushed immediately after installation. In addition, a lower gas flow during operation is beneficial to reduce the ageing rate. HV training on the other hand, can be used to restore the signal response, once part of the module has aged. Due to the higher voltage, high dark currents are produced which remove the insulating layer on the wire.

It is not always possible to repair all the damage using this method, since these currents are not necessarily located at the desired position [20]. Placing a source at the position with ageing forces the high currents at the correct place, repairing all the damage. It might be feasible to implement this procedure in the LHCb experiment, since the LHC beam can be used as source, which will automatically induce currents at the correct position.

Section 4.1 shows the setup used for both curing and ageing the module. Section 4.2 describes the results of curing with a source for two different ways of increasing the currents, by increasing the high voltage and by increasing the argon fraction in the gas mixture. To determine the optimal curing time, scans have been performed approximately every hour, results of which are shown in section 4.3. Finally the results of the effect of reversing the direction of the gas flow are shown in section 4.4.

4.1 Curing setup

To clean the wires, the currents have to be higher than normal. There are two ways to obtain higher currents. The first is increasing the high voltage, as is also done with regular HV training. The second method is the increase of the argon percentage in the gasmixture, since this increases the gain and thus the currents. The drawback of increasing the high voltage is that the detector can enter the discharge region and these discharges could in theory damage the wire. By increasing the argon percentage, the voltage can be kept lower to obtain the same currents. The latter method has also been tested in Heidelberg [37]. The gasmixture was changed from Ar/CO_2 70/30 to 90/10, while the high voltage was kept at the normal operating voltage (1550 V).

The curing method as conducted in Heidelberg is repeated. For this curing method the gas mixture will be changed to Ar/CO_2 90/10 and the voltage will be set to 1550 V. To compare

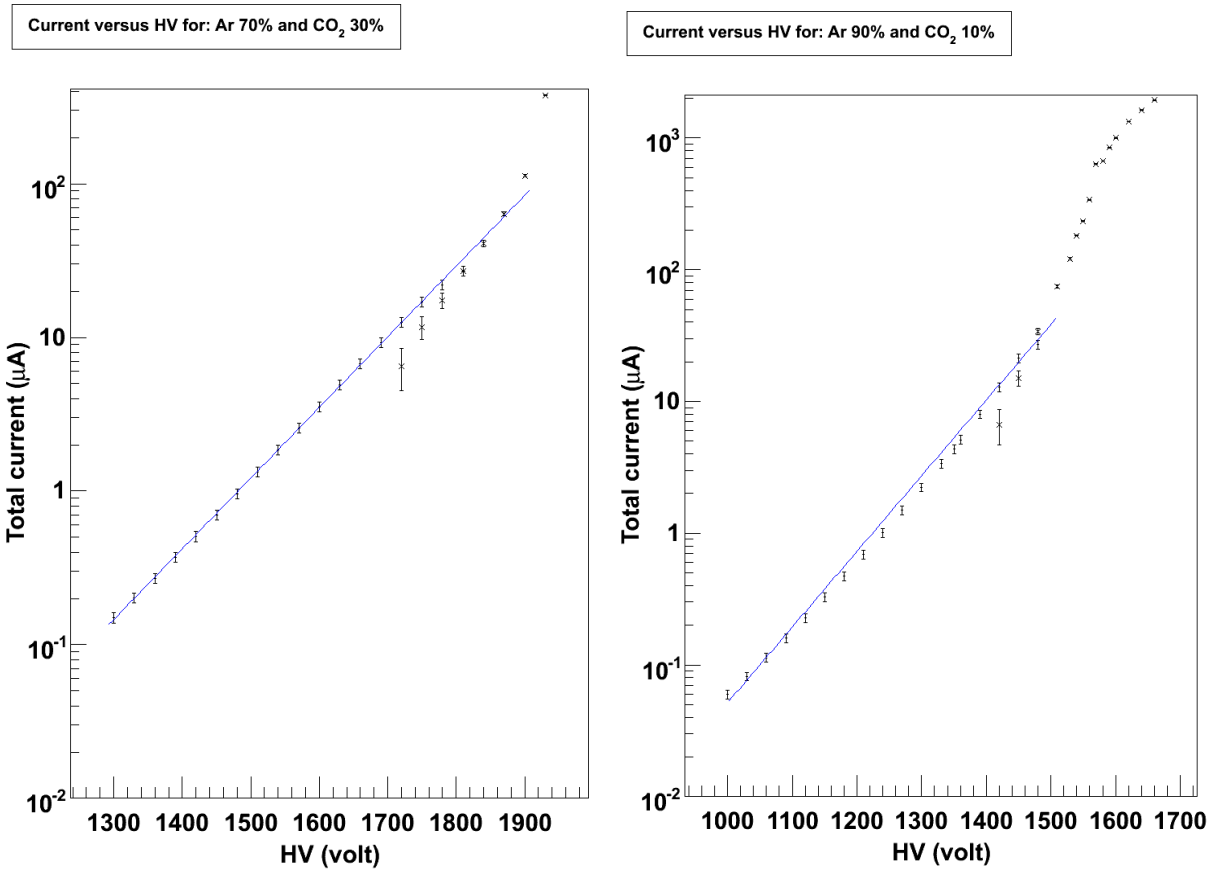

(a) (b)

Figure 4.1: *Total current summed over all 64 wires versus high voltage, with the nominal 20 mCi ^{90}Sr source illuminating the module: (a) Ar/CO_2 = 70/30 (b) Ar/CO_2 = 90/10.*

curing using a different gas mixture to curing at a higher voltage, a second curing method is tested. For this method the gasmixture will be the normal 70/30 mixture, but the high voltage is increased to obtain higher currents. Figure 4.1 shows the total current summed over all 64 wires versus high voltage. From figure 4.1(a) it can be seen that the current is about 2 μA at nominal gas mixture and voltage. From figure 4.1(b) it can be seen that at a gas mixture of Ar/CO_2 90/10 the detector enters the discharge regime around 1450 V, since the graph deviates from a straight line around that voltage.

The HV training procedure without a source induces dark currents in the module of about 10 μA [20]. To match these currents with a source, either the high voltage needs to be raised to about 1800 – 1900 V, or the argon fraction needs to be increased to about 90%, see figure 4.1.

A common way to obtain the gas gain of drift chambers is by measuring the response to a ^{55}Fe source. As explained in chapter 3, a ^{55}Fe source emits monochromatic photons with an energy of 5.9 keV which create a single cluster with on average 207 electrons. These primary electrons drift to the anode wire and result in a measurable pulse through gas multiplication.

The height of this pulse is a measure for the gas gain.

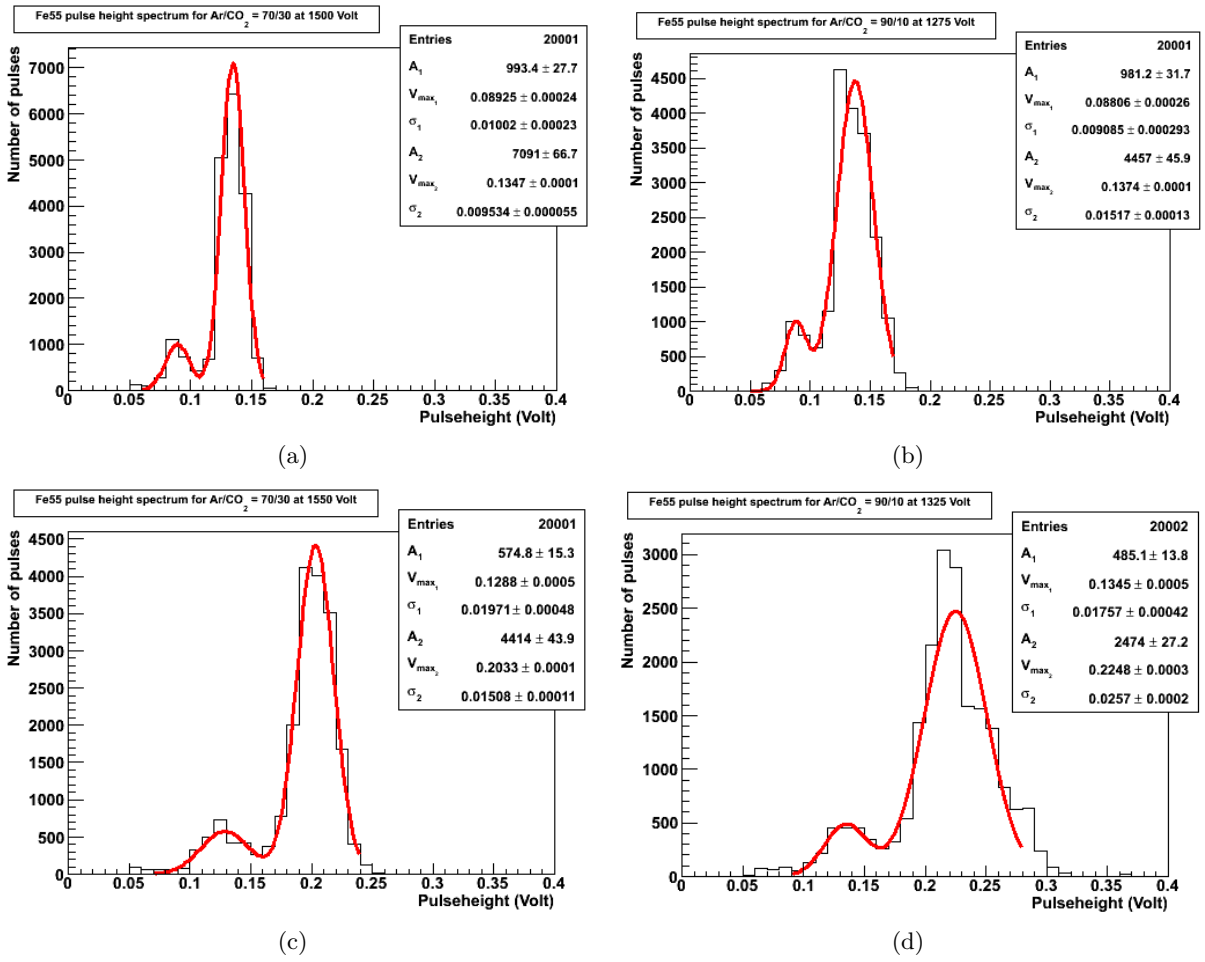

Figure 4.2: *Pulse height spectrum as measured with the ^{55}Fe source above wire 32 for (a) Ar/CO_2 70/30, 1500 V. (b) Ar/CO_2 90/10, 1275 V. (c) Ar/CO_2 70/30, 1550 V. (d) Ar/CO_2 90/10, 1325 V.*

Since all emitted photons have the same energy, a peak around a certain pulse height is expected. However, in the pictures shown in figure 4.2, two peaks are visible instead of one. The biggest peak is caused by the full absorption of the photons and is a measure for the gas gain. The smaller peak is known as the X-ray argon escape peak. Due to the energy levels of argon, it is possible that a secondary photon is created during the absorption of the photon emitted by the ^{55}Fe source. If this secondary photon escapes the straw tube, the deposited energy is lower, resulting in a secondary peak.

Figure 4.2 shows several pulse height spectra for both Ar/CO_2 70/30 and 90/10 for several values of the high voltage. These spectra are obtained by reading out the pulses induced by placing a 2 mCi ^{55}Fe source above wire 32 of module 121. The spectra are then fitted with a

double Gaussian:

$$N = A_1\, e^{(V-V_{max_1})^2/\sigma_1^2} + A_2\, e^{(V-V_{max_2})^2/\sigma_2^2} \tag{4.1}$$

with N the number of pulses, V the pulse height in Volt, A_1 and A_2 the heights of the left and right peak in figure 4.2 respectively, V_{max_1} and V_{max_2} the location of the peaks in Volt and σ_1 and σ_2 the half widths of the peaks in Volt.

The relative gain can be calculated by taking the ratio of the values of V_{max_2} for different gas mixtures or values of the high voltage [38]. From 4.2 it can thus be seen that the gain for Ar/CO_2 70/30 at 1500 V is approximately the same as the gain for Ar/CO_2 90/10 at 1275 V. It can also be seen that increasing the high voltage by 50 V increases the gain by about 55% for both gas mixtures.

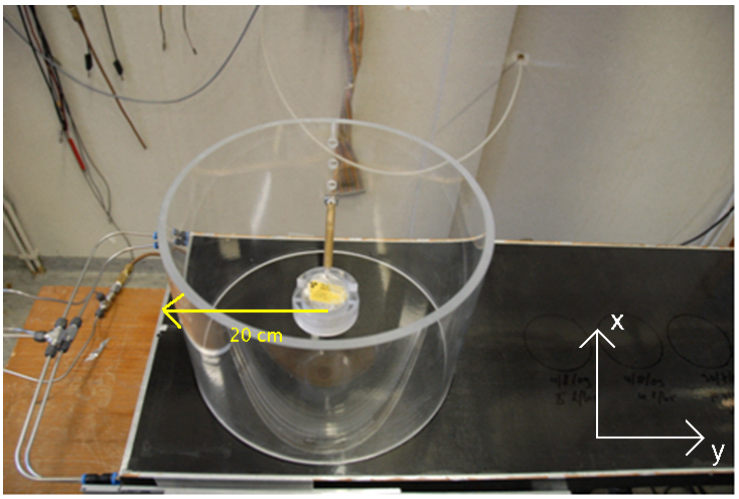

Figure 4.3: *Setup used for HV training with a source. This setup is also used to invoke ageing in the module.*

To cure the module, the setup as described in section 2.4 will be used. As explained earlier, this setup generates the same current profile as the LHC beam. The same source will be used to create the ageing as to recover the gain loss. A picture of the setup is shown in figure 4.3. The cylinder is placed above module 121 (S1 module) at x = 0 cm and at 20 cm from the end of the module, the gas flow will be 5 L/hr.

4.2 Results of curing at higher gain

Module 121 is first irradiated for 190 hours at 1550 V to create some damage, the results of which are shown in figure 4.4(a). In this picture the gas flow is from right to left. The big circle marks the location of the cylinder, while the small black circle marks the position of the 2 mCi source. After ageing the module, the damage is cured in three sessions. The details of these curing sessions are shown in table 4.1.

As a first test the high voltage was set to 1900 V and the module was cured for 17 hours. During this curing session, only wires 1 – 32 were connected. All the damage is repaired, as can

Table 4.1: *Details of the three curing sessions at higher gain conducted on module 121B.*

Curing session	Connected channels	HV (Volt)	Total current (μA)	Gas mixture (Ar/CO_2)	Total curing time (hours)	Shown in figure	Effect
1	1 – 32	1900	100	70/30	17	4.4(b)	✓
2	33 – 64	1800	28	70/30	6.5	4.4(c)	×
3	33 – 64	1550	220	90/10	6	4.4(d)	✓

be seen from figure 4.4(b). This was to be expected, since the high voltage is essentially as high as during normal HV training without source. The usage of the source forces the high currents to the right location.

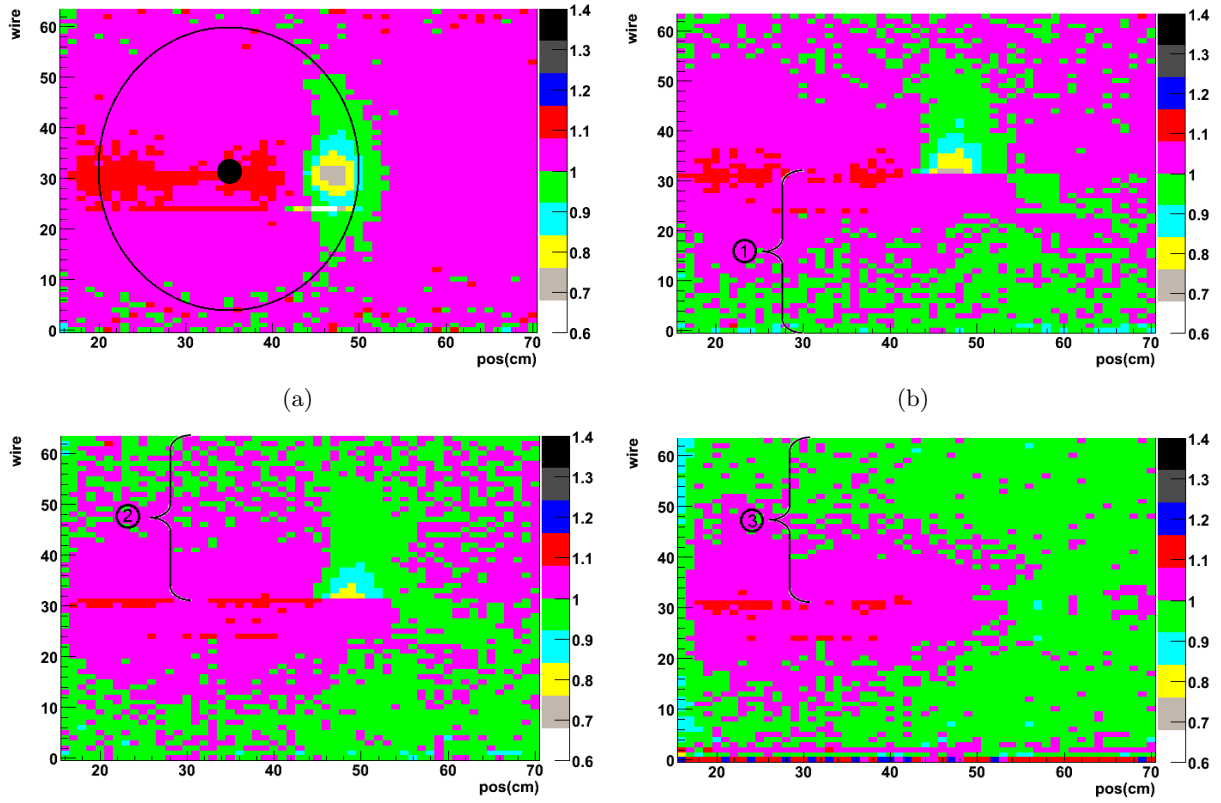

Figure 4.4: *(a) Result of ageing module 121 for 190 hours at 1550 V, the ellipse marks the location of the cylinder. (b) Result of curing module 121 at 1900 V for 17 hours: wires 1 – 32. The brace denotes the irradiated half. (c) Result of curing module 121 at 1800 V for 6.5 hours: wires 33 – 64. (d) Result of curing module 121 at 1550 V for 6 hours with Ar/CO_2 90/10 mixture: wires 33 – 64. [Module 121B, 25/11/2009 – 09/12/2009]*

As a second test, the voltage was set to 1800 V so that the currents are about 14 times higher

than normal. The module is cured for 6.5 hours, in order to have the same irradiation time as used in Heidelberg[1] [37]. For this test, only wires 33 – 64 were connected. Figure 4.4(c) shows the results of this curing and it can be seen that only some of the damage is repaired, with a relative gain increase of only about 8% (see also figure 4.5). Apparently, the currents were too low and the curing time was too short to remove the damage.

Since the damage of wires 33 – 64 was not repaired with the curing session at 1800 V, the same spot was monitored for the curing session using the Ar/CO_2 90/10 mixture. The high voltage is set to 1550 V and the module is cured for 6 hours. Figure 4.4(d) shows the results of this curing session, it can be seen that all the damage is repaired in this case.

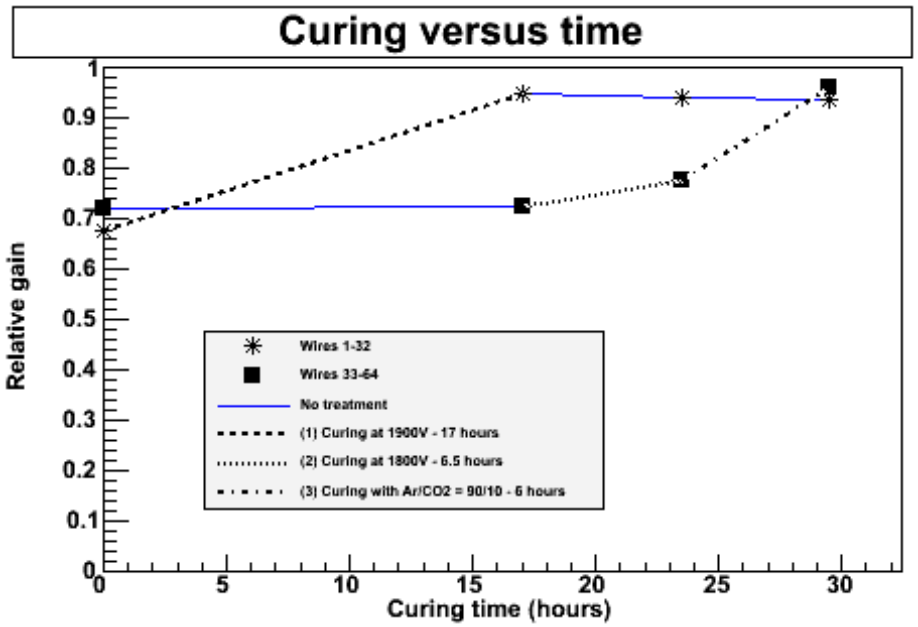

Figure 4.5: *Results of the different HV curing sessions.*

The results of the different curing sessions are summarized in figure 4.5. The time axis represents the time during which the module has been irradiated. Both groups of wires (1 – 32 and 33 – 64) are shown, but only one set was connected during each curing session. On the vertical axis the maximum gain loss at the aged spot on the module is shown, calculated using the minimum method. This figure shows that curing at 1800 V for 6.5 hours did not remove all the ageing. The gain only increased by about 8%. Curing the module at 1550 V for 6 hours using the 90/10 gas mixture did remove the ageing completely. The main difference between the curing sessions at 1800 V with the 70/30 gas mixture and 1550 V with the 90/10 gas mixture is the total current in the module as can be seen from figure 4.1 and table 4.1. So, it seems that the only relevant parameter for curing an aged spot is the current, which is confirmed by the result for the curing at 1900 V.

[1] In Heidelberg a curing at Ar/CO_2 90/10 was succesful in 6 hours, which was wrongly said to be at 20 times higher gain.

4.2.1 Ageing prevention after curing

After curing module 121, new damage is created at the same position by irradiating the module for 593 hours, with the normal 70/30 gas mixture restored. This time the module is irradiated at 1500 V, the result of this ageing session is shown in the top left picture in figure 4.7. An overview of the different ageing sessions conducted on module 121B is shown in table 4.2.

Table 4.2: *Details of the ageing sessions conducted on module 121B.*

Ageing session	High voltage (Volt)	Total ageing time (hours)	Shown in figure	Details
A	1550	190	4.4(a)	
B	1500	593	4.7(a)	After curing at higher gain

Figure 4.6 gives an overview of the development of the ageing of the module. Both ageing sessions and the curing sessions at higher gain (see figure 4.5) are shown here. The numbers denote the curing sessions as defined in table 4.1, while the letters denote the ageing sessions as defined in table 4.2. The time axis represents the irradiation time (both for curing and ageing). From the figure it can be seen that wires 1 – 32 start to age only after about 150 hours after the start of ageing session B, while wires 33 – 64 seem to start to age immediately. As described in section 2.3, the effect of ageing prevention after HV training of the wires at a high voltage has been observed before [20], but the details are not understood.

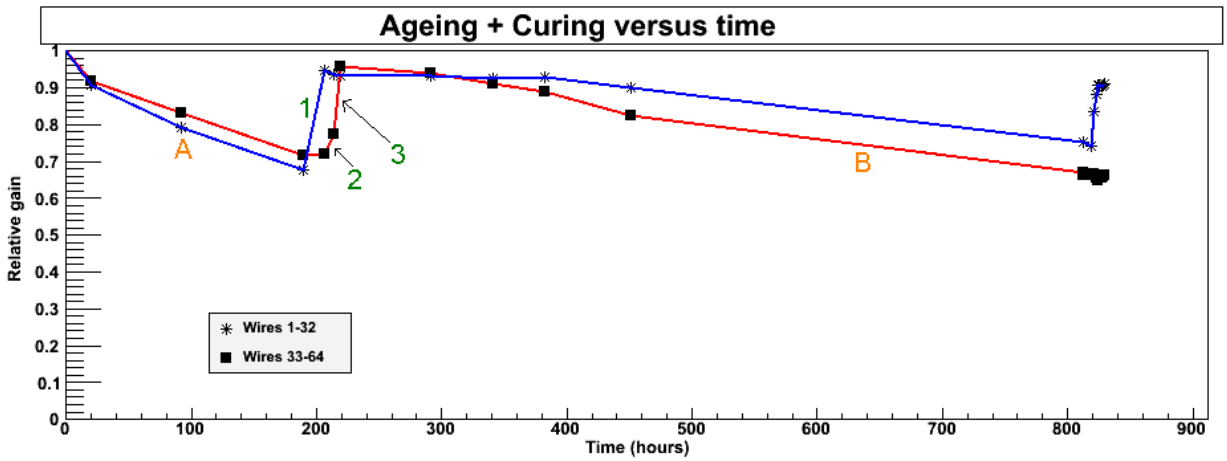

Figure 4.6: *Summary of module 121: first the module was aged for 190 hours (A), after that multiple HV curing sessions took place (denoted 1,2 and 3) and after that the module was aged again for 593 hours (B).*

4.2.2 Summary of curing at higher gain

Comparing the two curing methods it can be seen that both increasing the voltage and increasing the argon percentage repairs the ageing, provided the currents are high enough. The failure of

the curing session at 1800 V to repair all the damage lies in the fact that the currents are too low at that voltage. These measurements confirm that the only relevant parameter for curing an aged spot is the current. The advantage of increasing the voltage to cure the damage seems to be the prevention of subsequent damage. Also, it is easier to increase the voltage than to change the gas mixture of the Outer Tracker. Therefore it is recommended to increase the high voltage to cure damaged modules, rather than to increase the argon fraction.

4.3 Effect of the curing time

An important parameter for curing the aged modules is the curing time. The curing at 1900 V for 17 hours described in the previous section is a good example of this. After curing for 17 hours, all the damage was repaired. However, since no measurements are done in between, it is possible that the damage was repaired already after, for instance, 10 hours of curing.

To follow the gain increase in the time, scans of the module are made every 1 or 1.5 hours during the curing session to find the optimal curing time. For this curing, only wires 1 – 32 are connected and the high voltage is set to 1850 V. This voltage is chosen, since there are no dark currents [14], but it is still considerably higher than nominal.

Figure 4.7 shows the results of this curing session. From the scans it can be seen that most of the damage is repaired after 6 hours of curing. The graph with the relative gain calculated using the minimum method, which is shown in figure 4.8, confirms this. After curing more than 6 hours the gain only increases by a few percent[2].

Looking at the scans it can be seen that all the damage is essentially gone after curing, except for some damage located the farthest upstream from the source (the gas flow is from right to left). It appears to be very difficult to repair this damage, which can be understood from the fact that the currents are low far from the source, also because the plexiglass cylinder blocks the radiation from the source. To repair this last 10% of gain loss, it might help to reverse the gas flow, which is described in the next section.

[2]Wire 24 appears to age faster than the other wires, the reason for this is not understood. This wire is not taken into account when calculating the minimum gain for the graph in figure 4.8, but is shown separately. From the graph it can be seen that the damage in this wire is also repaired, although it takes somewhat longer.

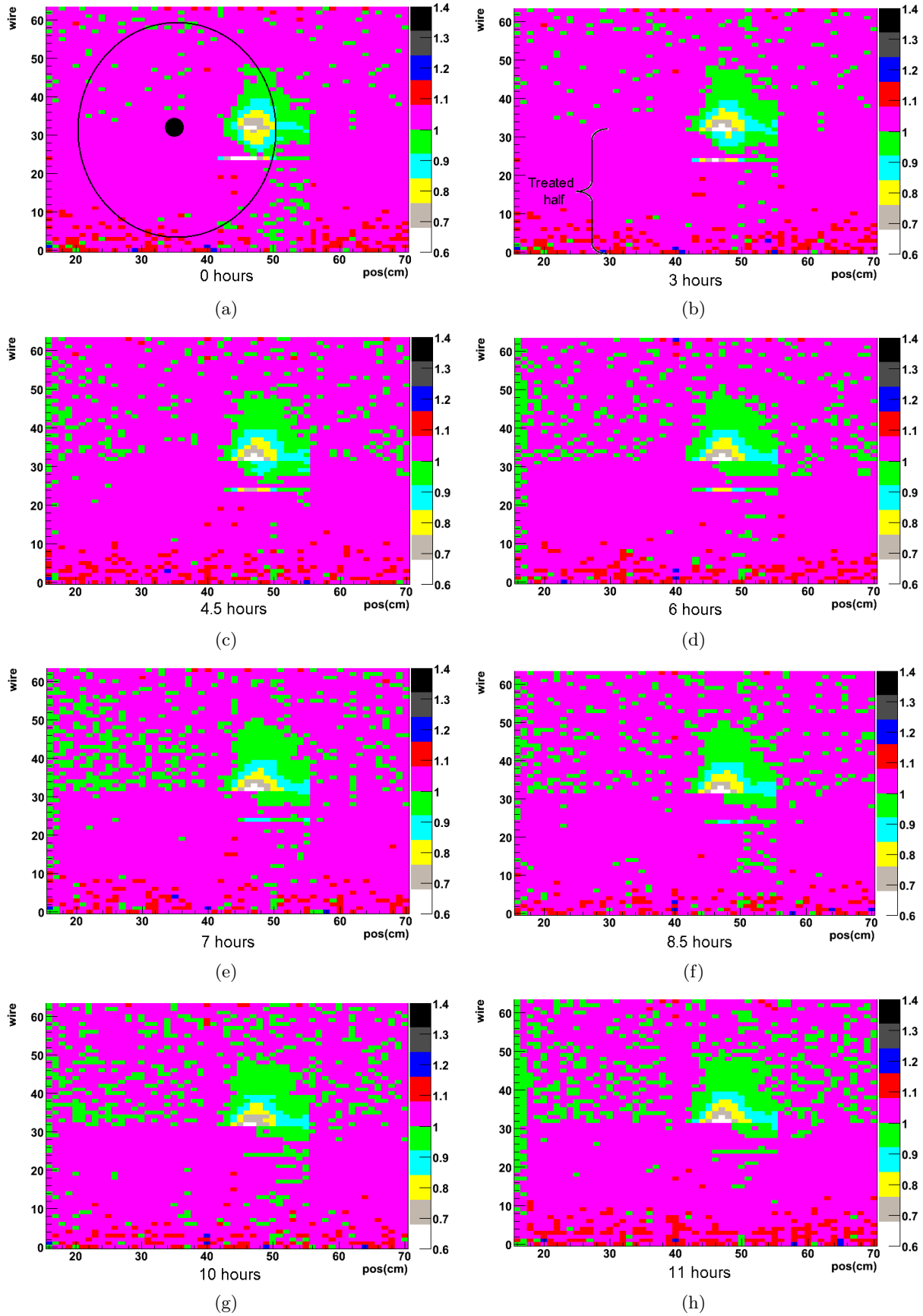

Figure 4.7: *Results of curing wires 1 – 32 at 1850 V, with scans of the module made regularly, the curing time is shown in the figures. [Module 121B, 27/01/2010 – 02/02/2010]*

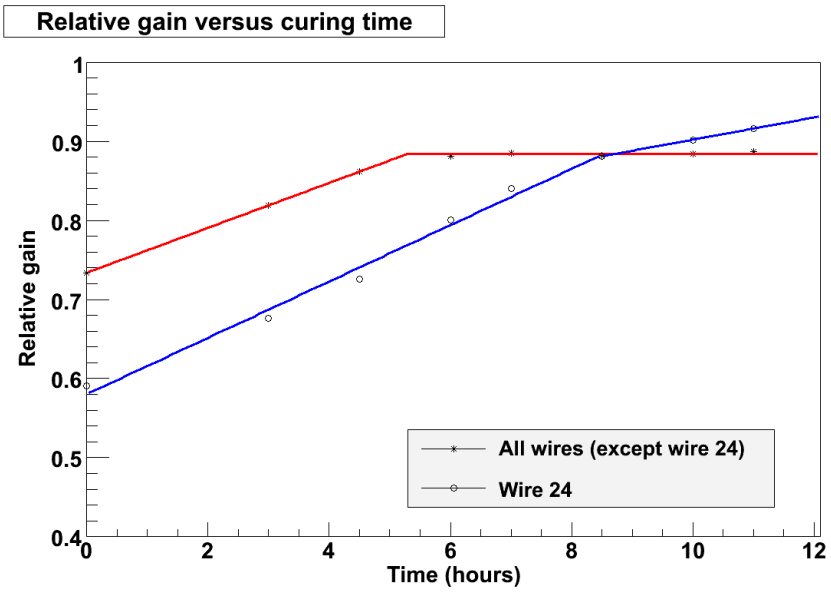

Figure 4.8: *Relative gain calculated using the minimum method versus curing time for the scans shown in figure 4.7. Wire 24 is shown separately since it behaves different from the other wires.*

4.4 Curing by reversing the gas flow

When ageing a module, damage is only created upstream of the source, the creation of damage downstream is prevented due to the production of ozone [39]. By reversing the gasflow, the damage will be located downstream of the source and could possibly be repaired by the created ozone. Reversing the gas flow would then also be able to repair the damage which is located the farthest upstream of the source in figure 4.7, which was not cured with the curing as described in the previous section.

The gas mixture will be the standard Ar/CO_2 70/30 mixture and the high voltage will be set to 1500 V. This curing session thus only implies the reversal of the gas flow and leaves both the high voltage and the gas mixture at the same values as during the creation of ageing (session B). Only wires 33 – 64 will be connected during this irradiation, since wires 1 – 32 have been cured already.

Figure 4.9 shows the scans of module 121 after different irradiation times. It can be seen that the damage which is now downstream (around 48 cm) slowly disappears in time. Also, new damage is created at the position exactly on the other side of the cylinder, now upstream of the source. The ozone that is produced due to the irradiation of the module not only prevents ageing downstream of the source, apparently it can also repair existing damage.

In figure 4.10 the relative gain, calculated using the minimum method, is plotted versus the irradiation time for both the old ageing spot and the newly created damage. Both graphs are fitted with a straight line and it can be seen that the curing and ageing rates are remarkably similar. This is unexpected, since curing and ageing are thought to be two entirely different processes.

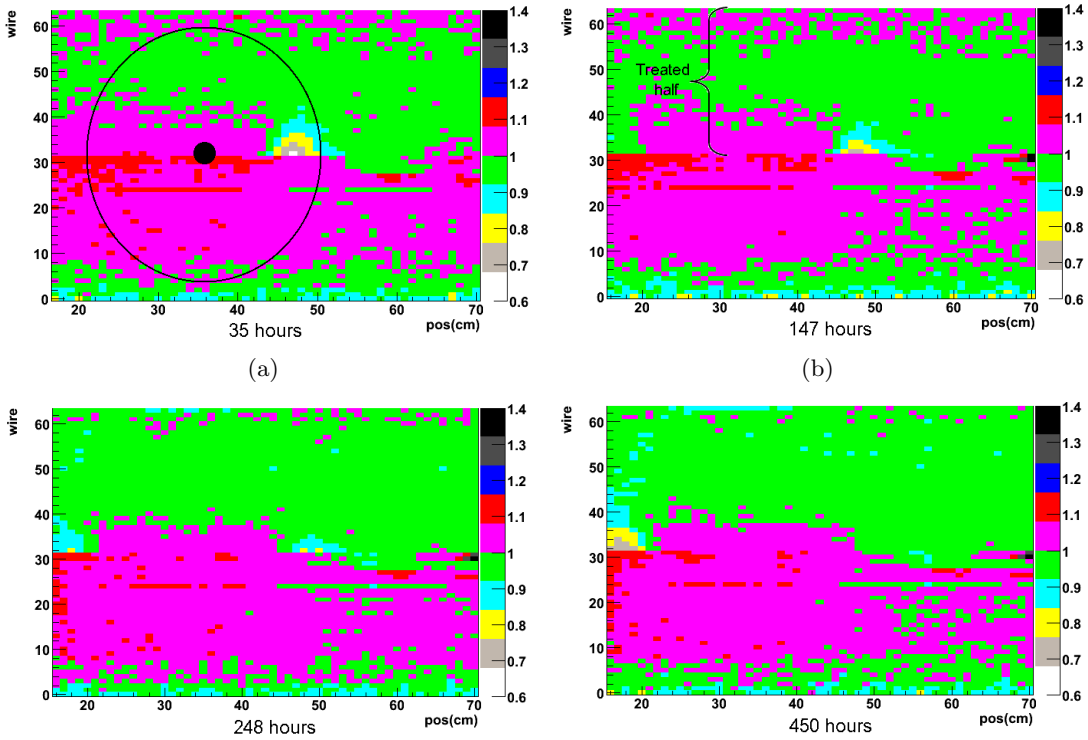

Figure 4.9: *Results of curing wires 33 – 64 after reversing the gas flow, which is from left to right in these pictures. Scans of the module have been made regularly, the irradiation time is shown in the figures. [Module 121B, 09/02/2010 – 08/03/2010]*

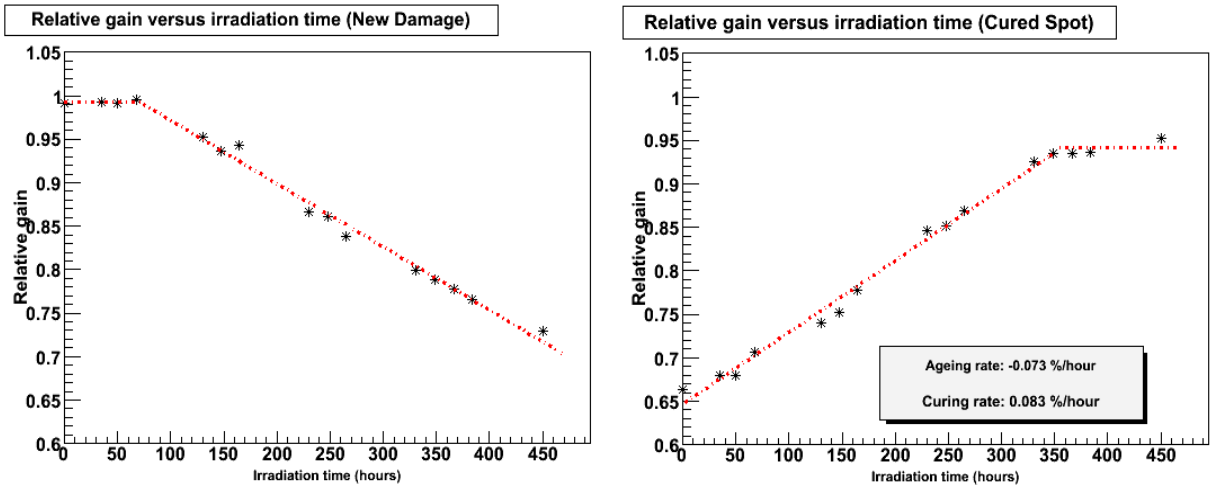

Figure 4.10: *Relative gain (compared to 0 hours of irradiation) versus the irradiation time for both cured spot and aged spot as shown in figure 4.9. Both graphs have been fitted with a straight line.*

Before curing wires 33 – 64 by reversing the gas flow, earlier gain loss of these wires was cured by irradiating for 6.6 hours at 1800 V, see also section 4.2 and figure 4.4(c). The prevention effect of this HV curing is visible in figure 4.10: the gain does not decrease during the first 80 hours.

4.5 Summary

An aged module can effectively be cured by increasing the currents and using a source to draw the currents to the correct place. The LHC beam can in principle be used as source, which was verified by experiments using a setup with an almost identical intensity profile as in the experiment.

In order to obtain higher currents, either the high voltage, or the argon percentage in the gas mixture can be increased. Both curing methods repair most of the damage if the currents are high enough, supporting the conclusion that the only important parameter for curing is the current. Curing the damage by increasing the high voltage appears to be favorable, since it will be easier to implement in the real detector and can prevent the creation of new damage.

Looking at the gain increase versus curing time, it appears that most of the damage is repaired relatively fast: at 1850 V most of the damage is repaired after 6 hours of curing; after 6 hours the gain stays approximately constant. Also, it is difficult to repair damage located far upstream of the source, presumably since since the currents are too low at that location.

A way to cure all the damage is to reverse the gas flow. By reversing the gas flow, damage that was first located upstream of the source will now be located downstream, which can then apparently be repaired by produced ozone. At the same time, new damage will be created on the other side of the source, at the same distance. The curing rate of the old damage and the rate at which new damage is created are surprisingly similar. The reason for this is not understood, since curing and ageing are different mechanisms.

However, the applicability of reversing the gas flow in the real experiment needs to be investigated, due to the different size of the irradiated area in the Outer Tracker.

Chapter 5

Monitoring ageing with final readout electronics

To determine if the Outer Tracker suffers from ageing effects, the modules are scanned in the laboratory with a ^{90}Sr source and the currents are measured, as described in chapter 2. The change of current is proportional to the gain variation caused by the ageing. In situ however, it is not straightforward to determine the gain loss, since the readout electronics measure drift times and do not measure pulse heights. In this chapter, a method is described to determine the amount of gain loss with the standard readout electronics, by means of a threshold scan.

Section 5.1 describes the threshold scan and how it can be used to determine gain loss in the OT modules. However, before the method can be used, it has to be calibrated first. This is described in section 5.2. Finally, the amount of gain loss predicted by the threshold scan is compared to the standard ^{90}Sr scan, to check the validity of the method. The results of this comparison can be found in section 5.3.

5.1 Threshold scan

The requirements of the Outer Tracker readout electronics are a precise and efficient time measurement to ensure single hit resolution and efficient charged particle reconstruction. Several tests have been performed on the readout electronics to make sure that this is the case [40, 41]. One of the tests that has been performed is the so called threshold scan, which is used to study the threshold characteristics.

As explained in chapter 1, the ASDBLR chip discriminates the induced pulse versus a set threshold. The unit of the threshold is the DAC, where 1 DAC equals 10 mV. The nominal value of the threshold in the OT is 80 DAC (or 800 mV), which corresponds approximately to a pulse with a charge of 4 fC. During a threshold scan, the threshold for all straws is varied and the hit efficiency is determined. For low values of the threshold, the hit efficiency will be 1, while for high values of the threshold it will be 0. In the absence of noise, the hit efficiency versus threshold would be a step function. In the more realistic case of Gaussian noise, the hit efficiency

as a function of threshold will be smeared and thus be given by an error function [42]:

$$P_{hit}(V_{thr}) = 0.5 - 0.5\,Erf\left(\frac{V_{thr} - HP}{\sqrt{2}\,\sigma_{noise}}\right) \tag{5.1}$$

where P_{hit} is the hit efficiency, V_{thr} the threshold value in DAC, HP the value of the threshold where the hit efficiency is 50% (called the half efficiency point) and σ_{noise} the width of the distribution in DAC. An example of a threshold scan for one straw is shown in figure 5.1(a), where the graph has been fitted with the function from equation 5.1.

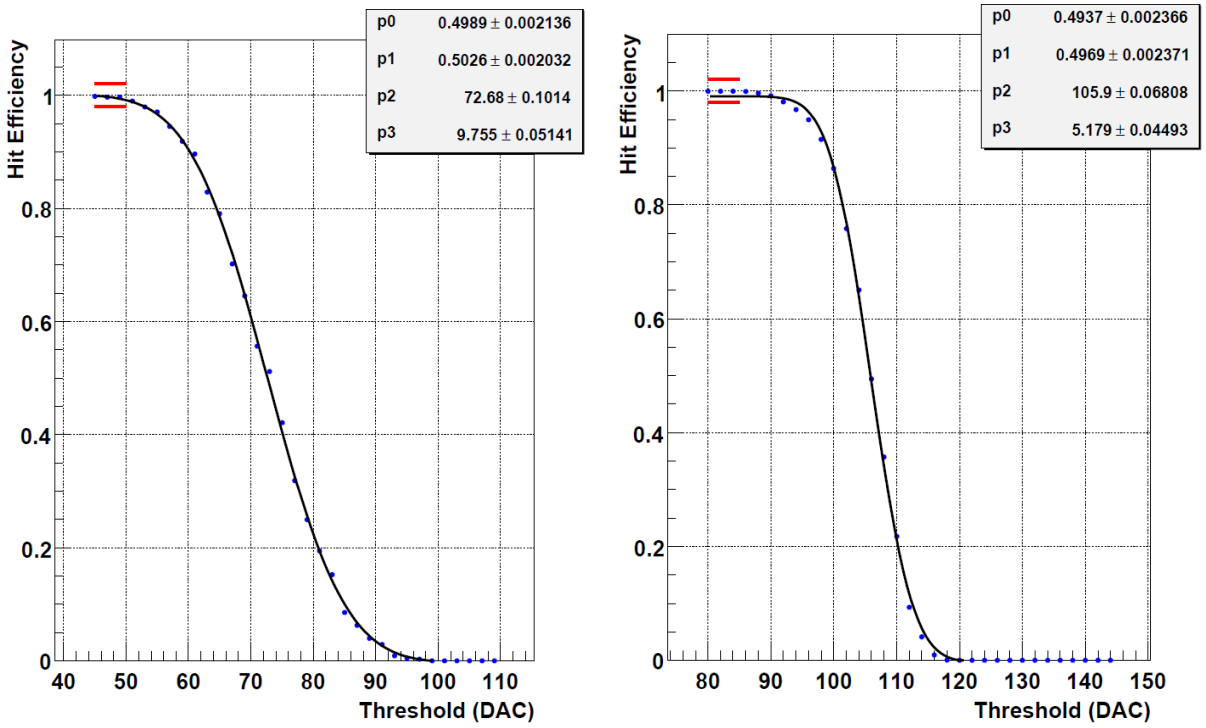

(a) (b)

Figure 5.1: *(a) Hit efficiency as a function of threshold for a low fixed input charge (3 fC). (b) Hit efficiency as a function of threshold for a high fixed input charge (8 fC).*

The channel to channel variation of the half efficiency point is supposed to be less than 6 DAC [40]. To check the uniformity, threshold scans at fixed charge have been done during production, using the test pulse signals (low and high injected charge) generated in the ASDBLR chip. Results of such a threshold scan for a single channel are shown in figure 5.1. It can be seen that the HP depends on the amount of charge that is injected. For a higher(lower) injected charge of about 8(3) fC, the value of the half efficiency point is approximately 106(73) DAC. This can be understood since a pulse with lower charge will be discriminated for a lower value of the threshold.

If ageing is present in the Outer Tracker modules, the amount of input charge will also be reduced, due to the insulating layer on the anode wire. By performing a threshold scan, it should

in principle be possible to determine the amount of ageing by looking at the shift of the HP. To do this, the method has to be calibrated first. When a shift of the HP is measured, it has to be converted in a relative gain loss. This will be described in the next section.

5.2 Calibration of the threshold scan

Before the threshold scan can be used to monitor the amount of ageing in the Outer Tracker it has to be calibrated, so that a given shift in the half efficiency point in a wire can be converted to an amount of gain loss. Section 5.2.1 describes the setup which is used for this calibration, and the results are then described in section 5.2.2 in the form of a calibration curve.

5.2.1 Setup

For the calibration, the same module (number 121B) will be used which has been used in chapter 4 for the HV training with a source. Instead of a current meter, a Front-End box (number FE442) will be connected to the module, which contains the readout electronics. A schematic of a FE-box is shown in figure 5.2(a) and a picture of a FE-box connected to an OT module is shown in figure 5.2(b).

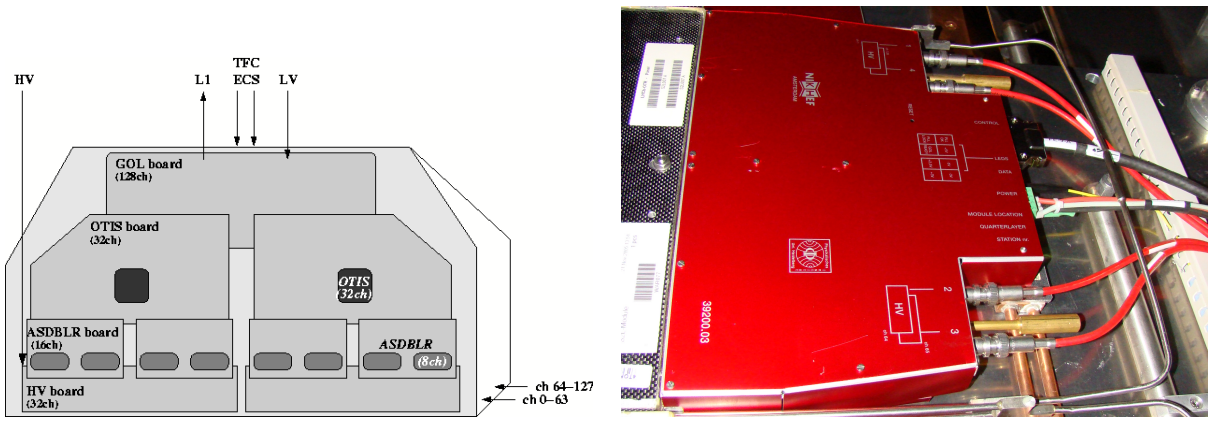

(a) (b)

Figure 5.2: *(a) Schematic of a Front-End box. (b) Front-End box connected to an OT module.*

During a threshold scan the threshold will be varied from 70 DAC to 160 DAC in steps of 2 DAC. At a threshold value below 70 DAC, the noise fraction rises above 1% [40], so lower values are not feasible. At a threshold of 160 DAC the hit efficiency will be 0 for all threshold scans done during the calibration.

The 20 mCi ^{90}Sr scanning source will be located above the center of the module and pulses from this source will be recorded. A total of 50000 events are read out at 40 MHz at every threshold step, without triggering on the electrons emitted from the ^{90}Sr source. Since no trigger is used, the hit efficiency will not start at a value of 1, but will start lower, since not every event will contain a hit in the straw tubes. Since the hit efficiency will not start at 1, equation 5.1

has to be modified to fit for the lower effective hit efficiency, which is proportional to the source intensity:

$$P_{hit}(V_{thr}) = 0.5\, P_{start} \left[1 - Erf\left(\frac{V_{thr} - HP}{\sqrt{2}\,\sigma_{noise}}\right)\right] \tag{5.2}$$

where P_{start} is the start value of the hit effiency. Table 5.1 summarizes the settings for the threshold scan.

Table 5.1: *Threshold scan settings.*

Start threshold (DAC)	End threshold (DAC)	Step size (DAC)	Number of events per step
70	160	2	50000

An example of a threshold scan at the nominal high voltage, 1550 V, is shown in figure 5.3. The results for two channels are shown, channel 5 is located near the edge of the module, while channel 22 is located near the center. The threshold curves look similar to those obtained for the test pulse, but the hit efficiency does not start at 1, as explained above. The start value of the hit efficiency is lower for channel 5 than for channel 22. This is due to the source profile, since the source intensity is highest at the center of the module.

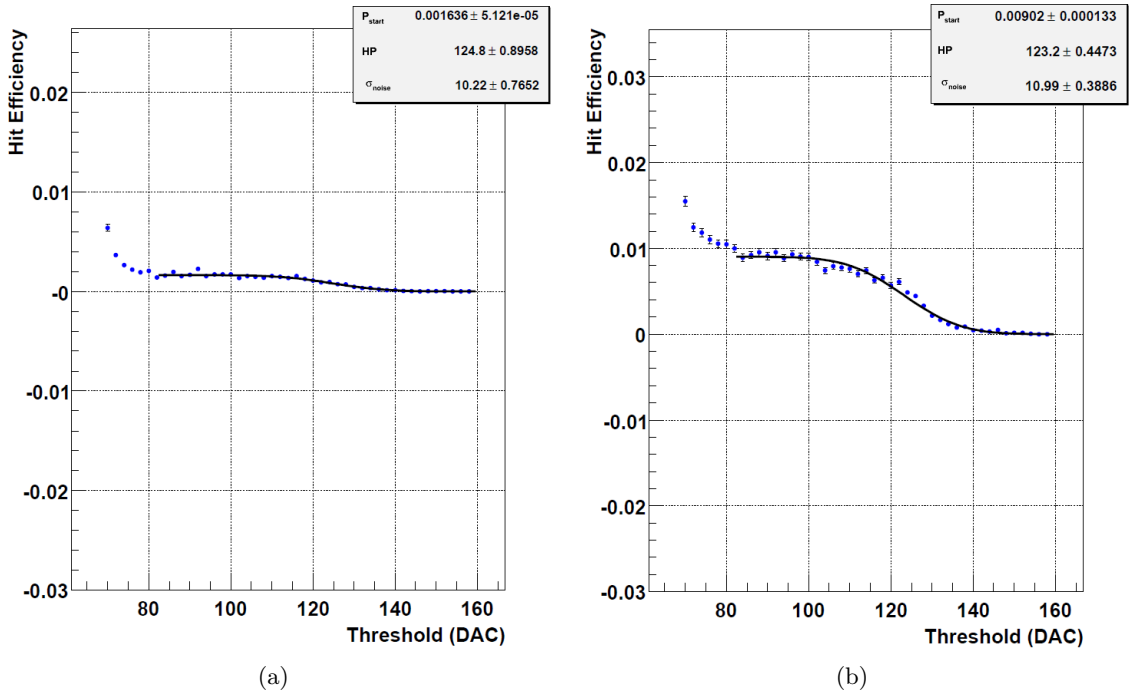

(a) (b)

Figure 5.3: *(a) Threshold scan of wire 5 of module 121B performed at 1550 V. (b) Threshold scan of wire 22 of module 121B performed at 1550 V.*

The values of the fit parameters for channels 5 – 59 are shown in figure 5.4. The other channels are not taken into account since the intensity of the source near the edges of the module is too low to obtain accurate results. In figure 5.4(a) the start value of the hit efficiency is shown for all channels under consideration, which resembles the source profile of the ^{90}Sr scanning source (see also figure 2.1(b)). Figure 5.4(b) shows the value of the HP versus channel, which is reasonably uniform for all channels, and ranges from about 120 DAC to 128 DAC at 1550 V. Finally, figure 5.4(c) shows the value of the width of the threshold curve versus channel, which also appears to be reasonably uniform for all channels. In the following paragraphs, only the value of the HP will be used.

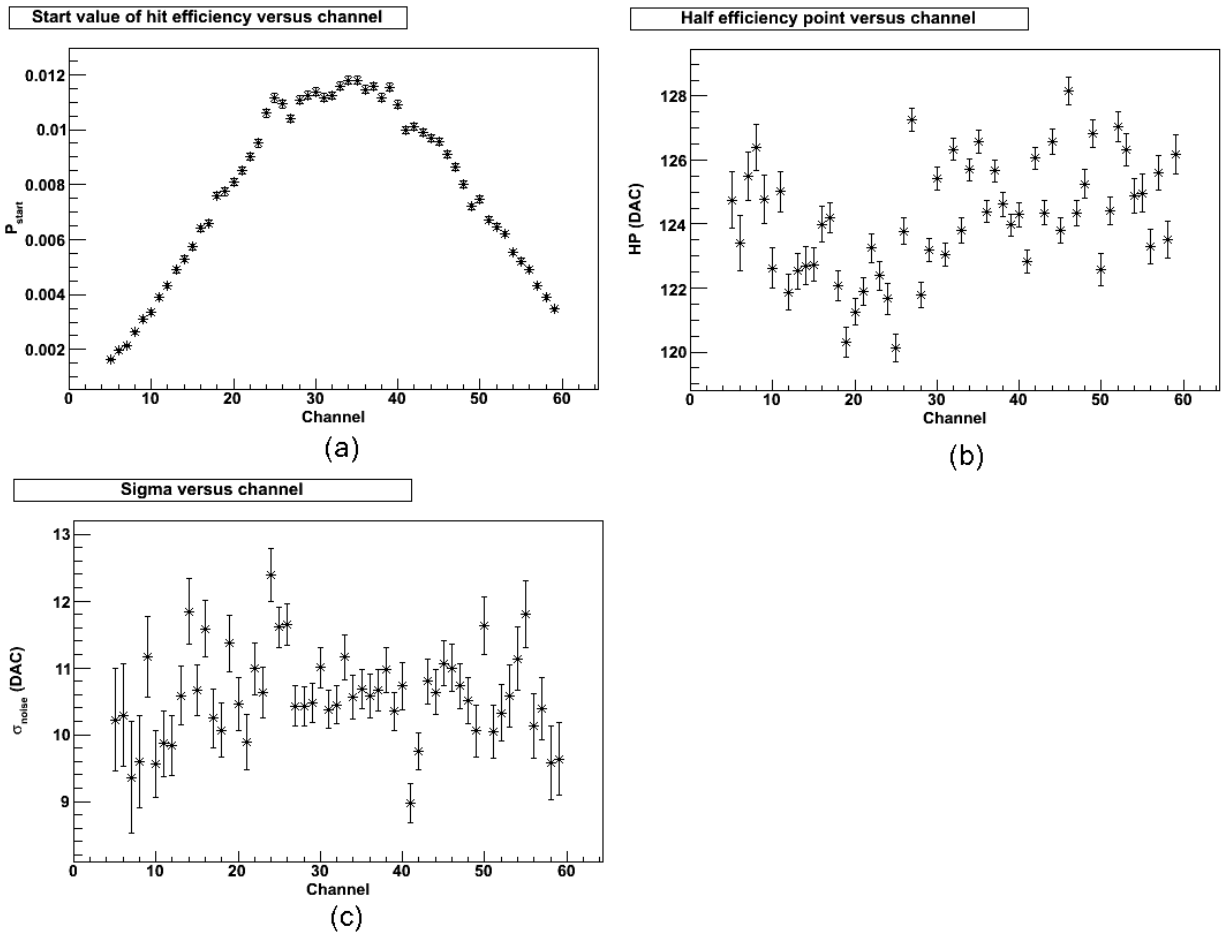

Figure 5.4: *(a) Start value of the hit efficiency versus channel. (b) Value of the half efficiency point versus channel. (c) Value of the width of the threshold curve versus channel.*

5.2.2 Calibration curve

To calibrate the threshold scan, the shift of the half efficiency point has to be measured as a function of the relative gain. By changing the high voltage applied to the OT module, the gain

can be varied. Table 5.2 shows the applied voltages and the corresponding value of the gain. (taken from [14]). Also the relative gain compared to the nominal value of the high voltage of 1550 V is given.

Table 5.2: *The HV values used to calibrate the threshold scan and the corresponding values for the gain [14] and relative gain compared to the value at 1550 V.*

High voltage (V)	Gain	Relative gain
1350	7872	0.122
1400	12999	0.201
1450	22358	0.346
1500	38141	0.590
1550	64605	1
1600	106685	1.651
1650	175700	2.720

A threshold scan will be performed at every voltage shown in table 5.2 and the shift of the HP will be calculated for channels 5 – 59 compared to the value of the HP at 1550 V. A histogram is then created for these shifts at every voltage and fitted with a Gaussian function. The results of this analysis are shown in figure 5.5.

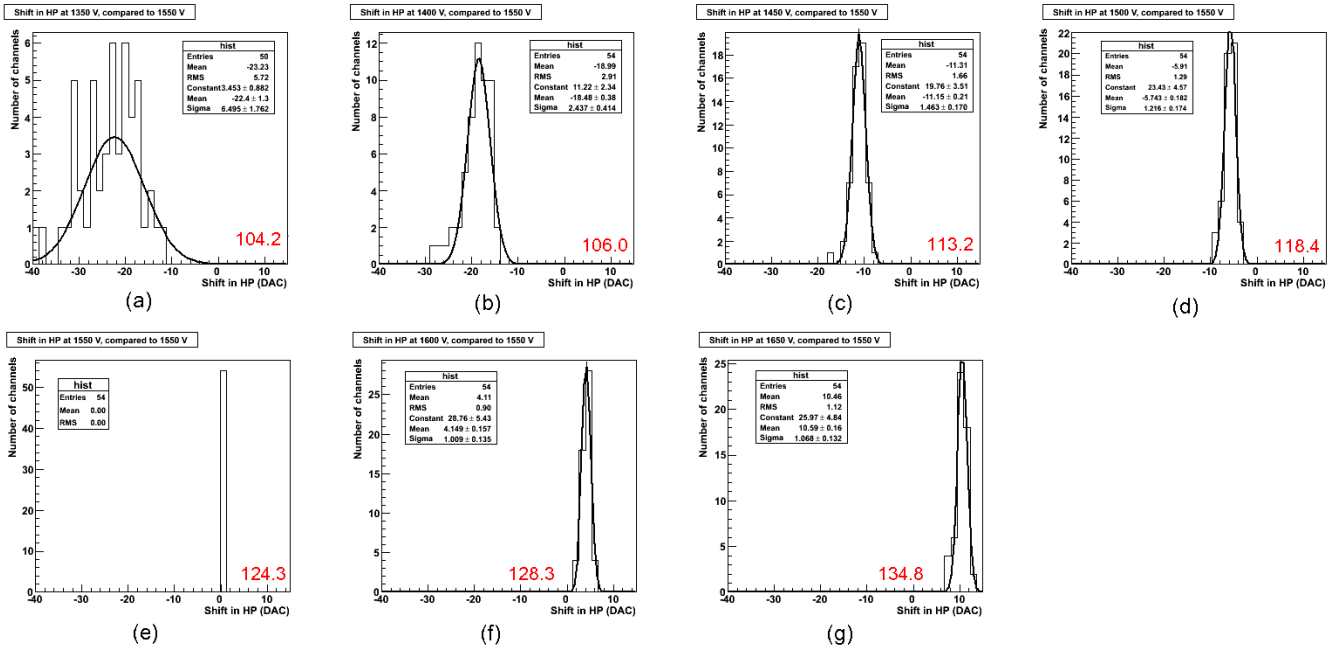

Figure 5.5: *Histogram of the shifts relative to 1550 V of the HP for channels 5 – 59 at a high voltage of (a) 1350 V. (b) 1400 V. (c) 1450 V. (d) 1500 V. (e) 1550 V. (f) 1600 V. (g) 1650 V. The mean absolute value of the HP is also shown for completeness. Note that by definition there is no shift of the HP at 1550 V.*

From figure 5.5 it can be seen that the Gaussian function fits the data well, which shows that the shift of the HP is quite uniform for all wires under consideration. The histogram at 1350 V is a bit worse because of the low absolute value of the HP, so that the contribution of the noise will be higher for that voltage. Also, the histogram at 1550 V is simply a delta function, since all shifts are calculated relative to this voltage.

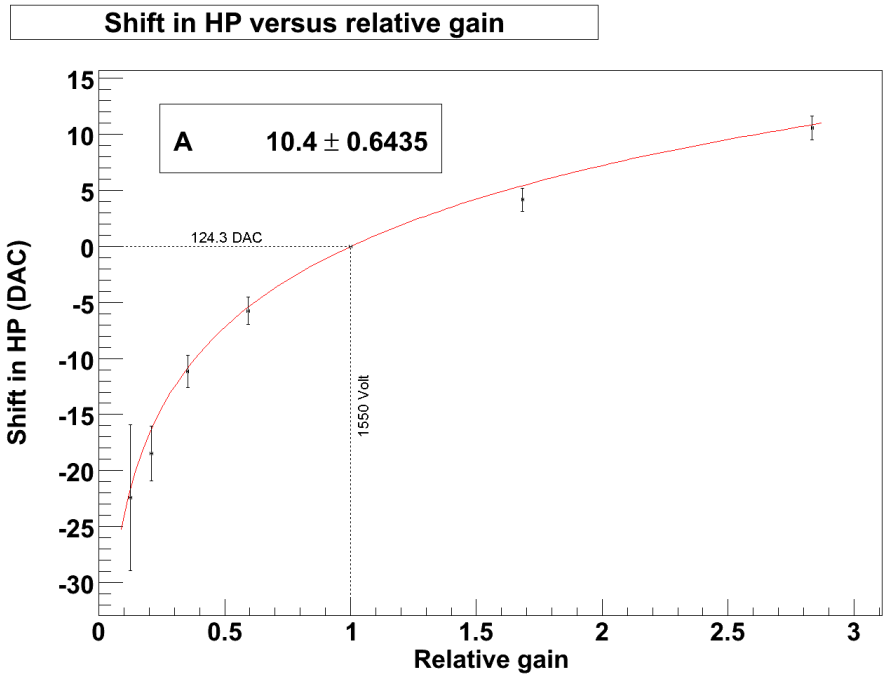

Figure 5.6: *Calibration curve for module 121B with the shift in half efficiency point versus relative gain. This curve can be used to calculate the amount of gain loss by measuring the shift in HP.*

By converting the values of the voltage to relative gain and taking the mean and the standard deviation (σ) of the fitted Gaussians, a calibration curve is made, which is shown in figure 5.6. It can be seen that a decrease in the HP implies a decrease of the gain and vice versa. This curve can be used to calculate the average amount of gain loss by measuring the shift in HP for a single channel. The calibration curve has been fitted with a logarithmic function:

$$\delta HP = A\, ln(G_{rel}) \tag{5.3}$$

where δHP is the shift in HP in DAC relative to the value of the HP at 1550 V, G_{rel} the gain relative to the gain at 1550 V and A the fit parameter. By inverting this function and using the value for A obtained from the fit, the relative gain can be calculated given a shift in HP:

$$G_{rel} = e^{0.096\,\delta HP} \tag{5.4}$$

It is important to note that only the average gain loss over an entire straw can be determined with this method, since a single value for the shift in HP is obtained per channel by performing a threshold scan. On the other hand, if no gain loss is observed on average, the average impact on the physics performance will also be small.

5.3 Comparison of the threshold scan with the ^{90}Sr scan

After calibrating the threshold curve, the method is compared to the standard way of determining the amount of ageing in an OT module (measuring the currents during a ^{90}Sr scan), to check the validity of the method. Both methods should give the same value for the amount of gain loss.

To check this, a spot with gain loss has to be created first. In order to accomplish this, the 20 mCi scanning source is placed at 35 cm along the module, which was irradiated for a total of 1046 hours at 1550 V. Only wires 1 – 32 were connected during this irradiation. The result of this ageing session after 1046 hours can be seen in figure 5.7, where the gas flow is from left to right.

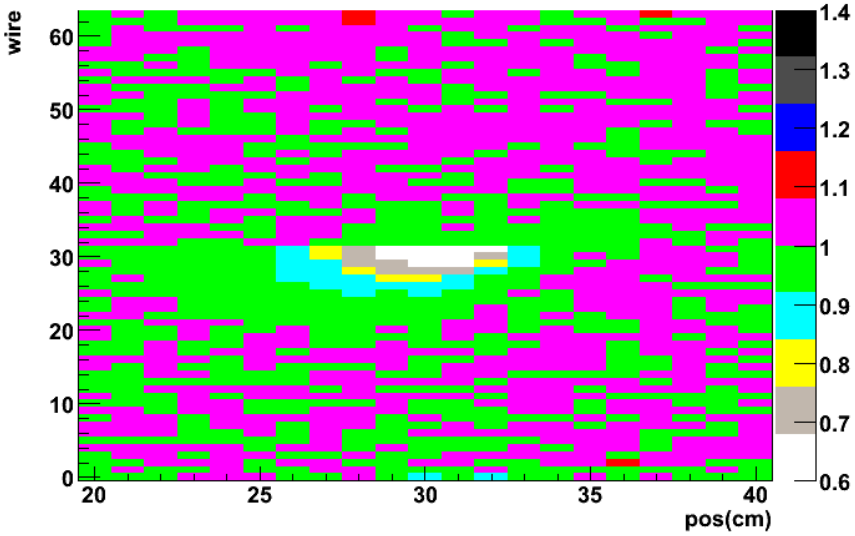

Figure 5.7: *Result of ageing module 121B for 1046 hours at 1550 V. Only wires 1 – 32 are connected, the gas flow is from left to right. [Module 121B, 07/05/2010 – 21/06/2010]*

From figure 5.7 it can be seen that the maximum gain loss is located around a position of 30 cm, which is downstream of the source as usual. To check the validity of the threshold scan, the scanning source will be placed at this location and a threshold scan will be performed at 1550 V, using the settings shown in table 5.1. The shift in HP will then be determined for channels 20 – 40 and formula 5.4 will be used to calculate the relative gain. To correct for differences in air pressure, which also influence the gain, wires 33 – 40 will be used to normalize the profile, since no gain loss is observed in these wires. The results for the relative gain for both the standard ^{90}Sr scan and the threshold scan are shown in figure 5.8 for several irradiation times.

From figure 5.8 it can be seen that both methods generally give the same value for the relative gain for all irradiation times, although the error on the values calculated using the threshold scan is a bit larger. This error is a combination of the error on the calibration parameter and the error on the determination of the HP for each channel and is dominated by the latter. The error on the relative gain determination with the ^{90}Sr scan is taken to be 2% for all channels. These results prove the validity of the method, so that the threshold scan can be used to monitor the

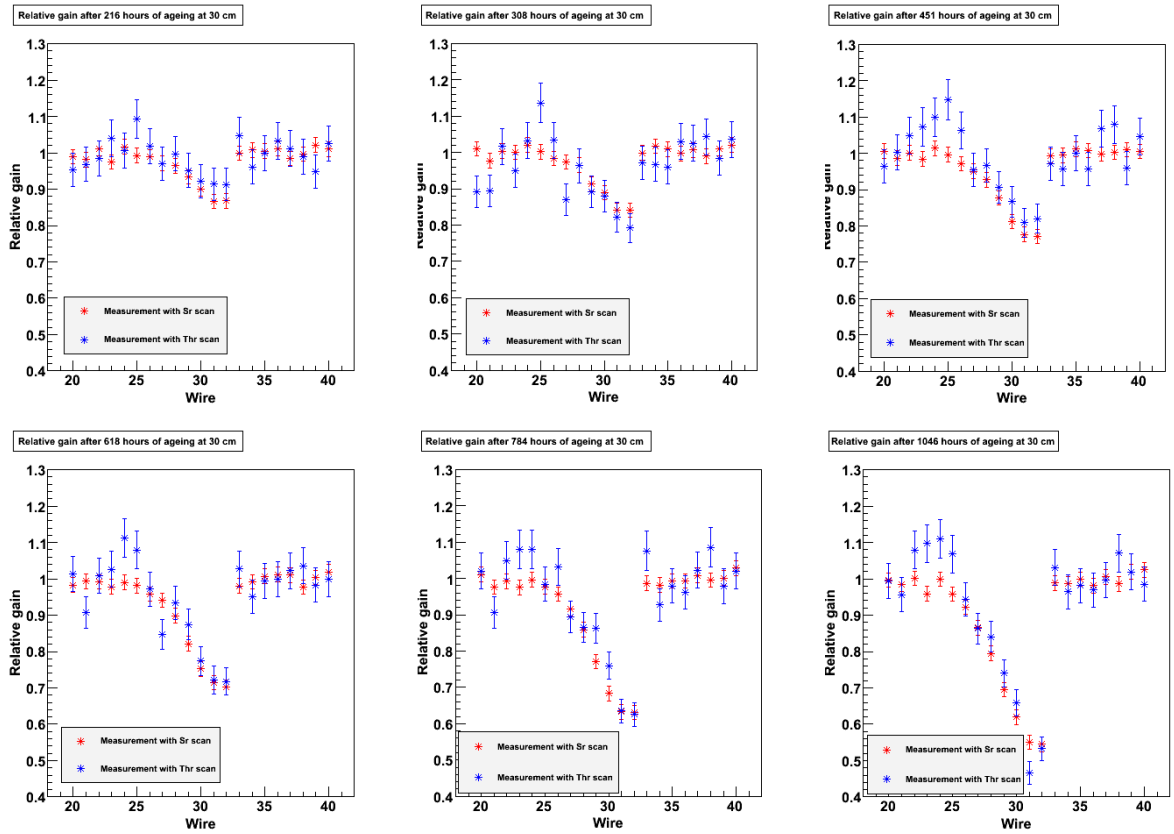

Figure 5.8: *Results for the determination of the relative gain at 30 cm along module 121B for both the ^{90}Sr scan and the threshold scan. Scans have been made after several irradiation times.*

amount of ageing in the Outer Tracker modules.

5.4 Summary

The standard way to monitor the amount of gain loss in the Outer Tracker modules is to perform a scan with a ^{90}Sr source. It is not straightforward to determine the gain loss in situ, since the OT readout electronics do not measure pulse heights.

By performing a threshold scan and looking at the shift of the half efficiency point, the amount of gain loss can be monitored using the readout electronics of the OT modules themselves. A decrease of the gain can be measured as a decrease of the half efficiency point of a channel. It has to be noted however, that only the average gain loss over the complete straw can be determined with this method.

By comparing the predicted amount of gain loss of the threshold scan with the values obtained using the standard ^{90}Sr scan, the validity of the threshold scan has been confirmed.

Chapter 6

Conclusion

The modules of the LHCb Outer Tracker have shown to suffer from gain loss under irradiation at moderate intensities, a process known as ageing. The plastifier in the Araldite AY103-1 glue used for the construction of the modules has been found to be the culprit, since it creates an insulating layer around the anode wire under irradiation. The effect of the plastifier in the Araldite AY103-1 glue has been examined by constructing a module with Araldite AY105-1. AY105-1 is identical to AY103-1, the only difference being that it does not contain the harmful plastifier. It has been verified that this module does not exhibit the same ageing problem. Even after an integrated dose of 0.18 C/cm/wire, which corresponds to about 3 years of OT operation, the maximum gain loss is only about 5%, which does not hinder detector operation.

Since it is not an option to rebuild all OT modules with AY105-1, other solutions have to be devised. There are three important aspects. First a way is needed to prevent ageing, secondly the ageing has to be monitored and lastly the ageing has to be cured if it occurs.

One way to prevent ageing is the addition of oxygen to the gasmixture, which has in fact been added to the Outer Tracker gas mixture. Because of its electronegative nature, oxygen can capture part of the drifting electrons, thereby lowering the signal and the efficiency of the OT straw tubes.

Simulations have been done using the GARFIELD and MAGBOLTZ programs, to check the effect of the addition of oxygen on minimum ionizing particles (electrons, as emitted by ^{90}Sr) and photons (emitted by ^{55}Fe). In both cases the addition of a few percent oxygen reduces the signal, but this does not hinder the operation of the Outer Tracker. The addition of 1.5% oxygen decreases the signal by about 16% for the detection of both electrons and photons. When comparing the simulated signal loss to the experimental values found for the Outer Tracker, it has been found that the simulated signal loss for ^{90}Sr is in reasonable agreement with the experimental values.

Besides reducing the signal, adding oxygen also increases the chance of not detecting a passing particle, which happens if all drifting electrons are attached. For minimum ionizing particles this effect is important, especially for tracks near the edge of the drift area. For an oxygen percentage of 1.5, roughly 1% of the minimum ionizing particles are not detected for the theoretical value of λ. Using the more realistic value of 850 μm for λ shows that on average 5.5% of the passing particles will not be detected, which is 1.5% worse compared to no oxygen. The inefficiency is

dominated by tracks near the edge of the drift area.

From the simulations it can be concluded that it is safe to add 1.5% oxygen to the gas mixture of the Outer Tracker, since both the signal loss and efficiency do not decrease such that it hinders detector operation.

The standard way to monitor the amount of gain loss in the Outer Tracker modules is to perform a scan with a ^{90}Sr source. It is not straightforward to determine the gain loss in situ, since the OT readout electronics do not measure pulse heights. By performing a threshold scan and looking at the shift of the half efficiency point, the amount of gain loss can be monitored using the readout electronics of the OT modules themselves. A decrease of the gain can be measured as a decrease of the half efficiency point of a channel. It has to be noted however, that only the average gain loss over the complete straw can be determined with this method. By comparing the predicted amount of gain loss of the threshold scan with the values obtained using the standard ^{90}Sr scan, the validity of the threshold scan has been confirmed.

Finally, a method exists to cure gain loss if present. This method is known as HV training and consists of increasing the applied HV such, that large dark currents will be induced in the straws. These currents can clean the wire, but do not necessarily occur at the correct location. By using a source to draw the currents to the correct place, an aged module can effectively be cured by increasing the HV. The LHC beam can in principle be used as source, which has been verified by experiments using a setup with a similar intensity profile as in the experiment.

In order to obtain higher currents, either the high voltage, or the argon percentage in the gas mixture can be increased. Both curing methods repair most of the gain loss if the currents are high enough, supporting the conclusion that the only important parameter for curing is the current. Curing the damage by increasing the high voltage appears to be favorable, since it will be easier to implement in the real detector and can prevent the creation of new damage.

Looking at the gain increase versus curing time, it appears that most of the damage is repaired relatively fast: at 1850 V most of the damage is repaired after 6 hours of curing; after 6 hours the gain stays approximately constant. Also, it is difficult to repair damage located far upstream of the source, presumably since the currents are too low at that location.

A way to cure all the damage is to reverse the gas flow. By reversing the gas flow, damage that was first located upstream of the source will now be located downstream, which can then apparently be repaired by produced ozone. At the same time, new damage will be created on the other side of the source, at the same distance. The curing rate of the old damage and the rate at which new damage is created are surprisingly similar. However, the applicability of reversing the gas flow in the real experiment needs to be investigated, due to the different size of the irradiated area in the Outer Tracker.

Bibliography

[1] P. Lefevre and T. Petterson, "The Large Hadron Collider: Conceptual Design," *CERN-AC/95-05*, 1995.

[2] LHCb collaboration, "A large Hadron Collider Beauty experiment, Technical Proposal," *CERN document CERN/LHCC/98-4*, 1998.

[3] I. Mous, "Aging in the LHCb Outer Tracker," Master's thesis, Vrije Universiteit Amsterdam, 2007.

[4] M. Blom, "Ageing of the LHCb outer tracker: Investigation of possible solutions and their effects on the detector performance," Master's thesis, Vrije Universiteit Amsterdam, 2009.

[5] A. D. Sakharov, "Violation of CP Invariance, C Asymmetry and Baryon Asymmetry of the Universe," *Journal of Experimental and Theoretical Physics Letters*, vol. 5, pp. 24–27, 1967.

[6] J. H. Christenson, J. W. Cronin, V. L. Fitch, and R. Turlay, "Evidence for the 2π Decay of the $K_2{}^0$ Meson," *Phys. Rev. Lett.*, vol. 13(4), pp. 138–140, 1964.

[7] M. Kobayashi and T. Maskawa, "CP-Violation in the Renormalizable Theory of Weak Interaction," *Progress of Theoretical Physics*, vol. 49(2), pp. 652–657, 1973.

[8] Belle collaboration, "Evidence for Direct CP Violation in $B^0 \to K^+\pi^-$ Decays," *Phys. Rev. Lett.*, vol. 93:191802, 2004.

[9] BABAR collaboration, "Observation of Direct CP Violation in $B^0 \to K^+\pi^-$ Decays," *Phys. Rev. Lett.*, vol. 93:131801, 2004.

[10] L. B. A. Hommels, *The Tracker in the Trigger of LHCb.* PhD thesis, Universiteit van Amsterdam, 2006.

[11] K. Kleinknecht, *Detectors for Particle Radiation second edition.* 1998.

[12] F. Sauli, *Principles of Operation of Multiwire Proportional and Drift Chambers.* 1977.

[13] L. B. A. Hommels on behalf of the LHCb Outer Tracker group, "The LHCb Outer Tracker Detector Design and Production," *LHCb Note OTR-2005-014*, 2005.

[14] V. Suvorov, G. Apeldoorn, I. Gouz, and T. Sluijk, "Avalanche and streamer production in Ar/CO_2 mixtures," *LHCb-2005-038*, 2005.

[15] LHCb collaboration, "Outer Tracker Technical Design Report," *CERN/LHCC/2001-024*, 2001.

[16] H. Deppe, A. Srowig, U. Stange, M. Feuerstack-Raible, U. Trunk, and U. Uwer, "The OTIS TDC Chip for LHCb Outer Tracker Readout," *LHC workshop proceedings*, 2004.

[17] S. Bachman *et al.*, "The straw tube technology for the LHCb outer tracking system," *Nucl. Instr. and Meth. A*, vol. 535, pp. 171–174, 2004.

[18] M. Capeans, "Aging and materials: lessons for detectors and gas systems," *Nucl. Instr. and Meth. A*, vol. 515, no. 1-2, pp. 73–88, 2003.

[19] S. Bachmann, Y. Bagaturia, M. Blom, L. Ceelie, D. van Eijk, C. Färber, T. Haas, I. Mous, A. Nawrot, A. Pellegrino, O. van Petten, E. Simioni, B. Storaci, M. Szczekowski, N. Tuning, U. Uwer, and D. Wiedner, "Ageing in the LHCb outer tracker," *LHCb-CONF-2009-019*, 2009.

[20] N. Tuning, M. Blom, D. van Eijk, I. Mous, A. Pellegrino, B. Storaci, and E. Visser, "HV Training as a Cure for the Ageing in the Outer Tracker," *LHCb-2010-009*, 2010.

[21] D. Wiedner, "Wire cleaning at nominal HV," *Presentation at LHCb Outer Tracker Meeting*, 08-03-2010.

[22] G. van Apeldoorn and N. Tuning, "Ageing Results from NIKHEF," *Presentation at LHCb week*, September 2006.

[23] J. Amoraal, "How much is the current in the OT," *Presentation at LHCb week*, November 2006.

[24] Huntsman Advanced Materials, "Araldite AY105-1 Safety Data Sheet." `http://www.resins-online.com/products-resin-support-products/products-l%atex.html?page=shop.getfile&file_id=122&product_id=222`.

[25] N. Tuning, "Glue investigations and irradiation of Tra-Bond module," *Presentation at LHCb Outer Tracker Meeting*, 25-05-2010.

[26] B. Storaci *et al.*, "Ageing Studies on an Outer Tracker Module Constructed with TRA-BOND Glue," *LHCb-2008-017*, 2008.

[27] M. Blom, I. Mous, and N. Tuning, "Effects of Adding Oxygen to the Outer Tracker Gas Mixture," *LHCb-2008-064*, 2008.

[28] `http://garfield.web.cern.ch/garfield`, 2008.

[29] S. Biagi, "A multiterm Boltzmann analysis of drift velocity, diffusion, gain and magnetic-field effects in argon-methane-water-vapour mixtures," *Nucl. Instr. and Meth. A*, vol. 283, pp. 716–722, 1989.

[30] `http://ref.web.cern.ch/ref/CERN/CNL/2000/001/magboltz`, 2000.

[31] R. M. van der Eijk, *Track reconstruction in the LHCb experiment*. PhD thesis, Universiteit van Amsterdam, 2002.

[32] H. Fischle, J. Heintze, and B. Schmidt, "Experimental determination of ionization cluster size distributions in counting gases," *Nucl. Instr. and Meth. A*, vol. 301, pp. 202–214, 1991.

[33] D. van Eijk. Private communication.

[34] M. Chefdeville, *Development of Micromegas-like gaseous detectors using a pixel readout chip as collecting anode*. PhD thesis, Universiteit van Amsterdam, 2009.

[35] D. Green, *The Physics of Particle Detectors*. 2000.

[36] H. Terrier on behalf of the LHCb Outer Tracker collaboration, "Performance of the Outer Tracker Detector of LHCb," *Journal of Physics – Conference Series*, vol. 110, 092031, 2008.

[37] C. Färber, "Outer Tracker Detector status," *Presentation at LHCb Outer Tracker Meeting*, 26-08-2009.

[38] G. van Apeldoorn, T. Bauer, E. van den Born, J. Nardulli, T. Ketel, A. Papadelis, A. Pellegrino, T. Sluijk, J. Spelt, N. Tuning, and P. Vankov, "Outer Tracker Module Production at NIKHEF - Quality Assurance,"

[39] C. Färber, "New results from ageing studies," *Presentation at LHCb week*, September 2008.

[40] A. Pellegrino, E. Simioni, T. Sluijk, A. Zwart, J. Schipper, P. Timmer, F. Jansen, N. Tuning, H. Terrier, T. Du Pree, A. Berkien, A. Weber, and P. Caputa, "OT FE-Box Test Procedures," *LHCb-2007-122*, 2008.

[41] F. Jansen, A. Pellegrino, T. Sluijk, H. Terrier, N. Tuning, and A. Zwart, "Linearity Measurements with the OTIS TDC for the Outer Tracker," *LHCb-2008-080*, 2008.

[42] L. Hommels, T. Bauer, A. Berkien, A. Pellegrino, and T. Sluijk, "Noise Studies with the LHCb Outer Tracker ASDBLR Board," *LHCb-2004-117*, 2004.